1976

Study of stress and temperature measured in the president costa e silva bridge (steel structure), M.S. thesis, May 1976.

David H. DePaoli

STUDY OF STRESS & TEMPERATURE MEASURED in the PRESIDENT COSTA E SILVA BRIDGE (STEEL STRUCTURE)

by

David H. DePaoli

A THESIS
PRESENTED TO THE GRADUATE COMMITTEE
OF LEHIGH UNIVERSITY
IN CANDIDACY FOR THE DEGREE OF
MASTER OF SCIENCE
IN
CIVIL ENGINEERING

May 1976

This thesis is accepted and approved in partial fulfillment of the requirements for the degree of Master of Science.

May 6, 1976
(Date)

Professor Alexis Ostapenko

Professor D. A. VanHorn
Chairman
Department of Civil Engineering

ACKNOWLEDGEMENTS

This research project was sponsored by Empresa de Engenharia e Construcao de Obras Especials of Rio de Janeirio, Brazil.

Special thanks go to Dr. A. Ostapenko, my thesis advisor, without whose help this thesis would not have been possible. Others who aided in my work are Dr. J. W. Fisher, Mr. H. T. Sutherland, and Mr. J. E. O'Brien. I would also like to thank the secretaries in the Word Processing Center for typing the manuscript, the drafting staff for their excellent work and Mr. Richard Sopko for his aid in preparing the photographs.

Table of Contents

List of Tables

FIGURE TITLES

Figure Titles (cont'd)

ABSTRACT

This thesis traces the record of strain changes, stress changes and moment variations of the steel portion of the Presidente Costa e Silva Bridge in Brazil. Three stress and strain change phases are discussed; 1) construction, 2) test loading, 3) thermal.

Data from three measurement systems - electrical strain resistance gages, a mechanical strain gage, and scratch gages - were used to analyze the stress and strain distributions in cross sections and the moment variation along the bridge. These distributions were used along with construction information, loading data and temperature variation data to; 1) evaluate construction stress changes ("stress change" refers to a change in stress condition, not the actual stress condition) for any possible danger signs, 2) assure the long term safety of the bridge.

As expected, construction stress changes, up to 250 MPa (2550 kg/cm) were of the order of five times greater than any other measured stress changes, and showed close agreement with theoretical stress changes thus the bridge was not overstressed during construction. Apparent daily thermal stress changes up to 52 MPa (525 kg/cm^2) were measured. Traffic loading was found to have a negligible effect on the gross stress condition of the bridge.

Also, stress change measurements led to the finding that the location of the neutral axis of the structure is somewhat at variance with the design location.

1. INTRODUCTION

1.1 General

Dedication of the Presidente Costa e Silva Bridge took place on 4 March 1974, after nearly five years of work. The bridge carries six lanes of traffic over the Guanabara Bay between the cities of Rio de Janeiro and Niteroi in Brazil (see Fig. 1), providing an alternative to either a 2½ hour round trip around the bay or a ferry ride. The bridge, at 11 km (9 km over water), is the world's fifth longest road crossing.

The opening of the bridge was the culmination of a century of planning on the spanning of Guanabara Bay - an economic and social necessity for Brazilians living in one city and having ties (work, commerce, family) with the other. Several other concepts, including a tunnel and a suspension bridge, had been rejected as impractical or too costly.

Except for the central portion, the bridge is constructed of post-tensioned concrete box girder sections. The 848-meter central steel box girder portion incorporates the world's longest unstayed steel box girder span of 300 meters.

The massive steel span was necessitated by a 300-meter minimum clearance for the main shipping channel, and a limiting

construction depth of 12.4 meters which resulted from two constraints. The first constraint was a shipping headroom requirement of 60 meters above mean water level. The second constraint was a 72.4-meter maximum height restriction due to the presence of an airport a few kilometers away.

The steel structure consists of an orthotropic steel deck (25.8 meters wide) integral with the main girders, and two box girders (each 6.86 meters wide). The depth of the box girders varies from 4.69 meters at the junctions with the concrete approach spans, to 13.05 meters over each central channel pier.

The design was carried out by Howard, Needles, Tammen and Bergendoff International (HNTB) of Kansas City, Missouri. The steel was fabricated and erected by the joint venture of Redpath Dorman Long, Ltd., and Cleveland Bridge and Engineering Co., Ltd., and Montreal Engenharia S.A. A Rothchild load requirement stipulated that British steel be used. As a result, the steel, 8000 tons of the 13000 tons being of 402-447 MPa (4100 - 4560 $kg.cm^2$) yield strength was fabricated in England and shipped in pieces to Rio. The steel pieces were then assembled into seven units at Caju Island (Fig. 1), floated to the piers, and jacked into place.

1.2 Scope of Field Study

The Lehigh field study was undertaken for several reasons. Several similar structures had failed, and a guarantee of the safety of the structure was desired. A check on the design assumptions was deemed necessary; this included an evaluation of construction stresses due to the novel construction techniques, and measurements of traffic load distribution. Also, a check on traffic durability and possible fatigue effects was needed, and a measure of temperature change effects on the bridge.

This thesis discusses the force history of the steel portion of the bridge, and the conclusions formulated therefrom. The force history is the record of the effects of stress changes and strain changes on the bridge. The presentation is in three parts; the construction sequence investigation, the test loading investigation, and the thermal effects investigation.

1.3 Construction Sequence

The steel erection phase (see Fig. 2) took place in three massive lifts (two double side span lifts and the center span lift) and two smaller lifts (of the suspended 44-meter spans). The seven separate units (four haunched half sidespans, center span, and two smaller suspended spans) were constructed

on Caju Island near the bridge, floated out to the piers, and jacked into place on lifting assemblies.

First to be constructed was the center section of the steel main span, 176 meters in length and weighing 34,700 kN (3900 tons). This unit was then used as a barge to float the four side span units to the lifting assemblies.

The side span units were assembled along side each other so as to prevent misalignment. Each side span was then separated along its longitudinal center line and each half side span, 292-meters long and weighing 22,000 kN (2500 tons), was moved transversely out to the pontoon. The units were then floated out the jacking assembly at the bridge piers.

The jacking assembly consisted of steel box ring girders around the bottom of each pair of pier shafts, steel jacking columns and 450-ton double-acting hydraulic jacks. Each side span unit required six jacking columns and twelve jacks grouped in pairs.

After the two lifts of the four half side span units (one lift of the two Rio side span units and one lift of the Niteroi side span units), each pair of units was joined together. The jacking columns were then moved to the ends of the haunch cantilevers for the center span lift.

As the center span was lifted out of the water, it assummed a virtually stable shape. Lateral stability was maintained through transverse tackles attached to the piers, and aerodynamic oscillations were controlled by damping gear installed from the cantilevered ends of the side spans. Once the center span was in place, the cantilevered end of the Rio side span was jacked up for alignment, and tie bolts were used to splice the top flanges and a three-span continuous structure was formed.

2. INSTRUMENTATION

2.1 Location of Instrumentation

The north and south boxes of the Rio side span were chosen for instrumentation. (Also, one scratch gage was installed in the north box of the center span after completion of bridge construction.) Six floor beams were instrumented: FB (floor beam) 17, FB27, FB42, FB51, FB57 (north and south boxes for all five), and FB87 (north box only). (See Fig. 3 for locations.)

FB17 was chosen for instrumentation for two reasons. First, it is one of the pier locations of the side span. Second, it was subjected to statically determinate moment changes.

Two primary reasons also resulted in the choice of FB27 for instrumentation. First, a typical braced frame cross section was needed to study transverse bending. Second, for the temperature study, an average depth cross section within the span (not encumbered by the presence of piers) was needed.

Floor beam location 42 was chosen for instrumentation for two primary reasons. First, a moment measurement was desired near midspan. Secondly, it was desired to study the deformation of the cross sectional shape due to asymmetrical loading, and,

as FB42 has no cross bracing, and is halfway between two braced sections, it was felt that this location would provide the best information.

Floor beam location 51 was chosen primarily because it is the transition location from straight line section variation to haunched section variation. It is also one of the deeper cross sections. At this location, the concentration was on the shear stresses, and the bending stresses in the top and bottom flanges. Most of the gages at FB51 were in the north box, however there were a few placed in the south box.

Floor beam location 57 was chosen for instrumentation for the following reasons: 1) FB57 is the largest section, is an end pier location, and has the sharpest haunch effect, 2) it was expected that warping stresses at this location would be most pronounced, 3) FB57 was one of the locations instrumented for the temperature study, as it is located directly over a pier. As such, FB57 was the most instrumented section.

Ideally, the center of the diaphragm of each floor beam would have been the instrumented location. However, the instrumented locations were 40-50 cm off the center line so the effects of details and connections would be neglibible according to St. Venant's principle. (2 to 3 times the clearance between the troughs - 18 cm - was taken as the critical distance.)

The decision to locate gages on a specific side of the floor beams was based on the following reasons:

FB17: The gages were placed on the Rio side to take advantage of the static determinacy of the cantilever for both moment and shear.

FB27: The Niteroi side was chosen because of a splice on the other side that might have caused local disturbances. Also, a special internal bracket was temporarily placed on the Rio side to avoid load overstressing when the girders were transported on the pontoons.

FB42: Since a scaffold had to be built to monitor dynamic stresses at a splice on the Rio side, it was decided to take advantage of the scaffold and place the gages there.

FB51: Not only temporary erection brackets but also a reinforcement truss caused local disturbance of the Rio side, thus the Niteroi side was chosen.

FB57: The Rio side was selected so that the data could be correlated with the analysis of other sections under study in the span.

2.2 Description of Gage Systems

Three separate types of stress and strain measurement gages were employed: electrical resistance gages, scratch gages, and a mechanical gage system. Each system was chosen for certain individual merits, these merits complementing each other so as to provide the most complete force history of the bridge.

The electrical resistance gages first provided a record of strain changes during the construction sequences. They were used in subsequent studies, in conjunction with temperature gages, to provide an account of temperature changes and strain changes throughout the day. Scratch gages were used to provide continuous records of stress changes over long time periods, and to provide a backup system in case the electrical gage system was not functioning properly. The mechanical gage system provided an account of total strain changes from the time of one set of readings until the time of another set.

Prior to the field splice on 5 Jan 74, connecting the side spans to the center span, the side span units were statically determinate structures. Stress and strain changes computed from all three measurement systems were proportional by the modulus of elasticity of the steel - 2.06×10 MPa (2.1×10 kg/cm). The field splice made the structure statically indeterminate.

The electrical and mechanical systems then measured strain changes (but not necessarily stress changes) while scratch gages measured stress change (but not necessarily strain changes).

2.3 Electrical Gage Systems

The electrical gage system provided the most accurate data of the three systems. It included both strain and temperature gages. Strain gages were installed at FB17, FB27, FB51, FB57 on both the north and south boxes, and temperature gages were installed at FB27 and FB57 on the north and south boxes. The strain changes for the first two construction sequences were recorded by a Datran* data recorder. Subsequent strain and temperature changes were recorded by a B&F** data recorder positioned first in a shanty and later on a truck, on top of the bridge. A summary of the times when electrical gage readings were taken is in Table 1.

2.4 Scratch Gages

Scratch gages provide a permanent and continuous record of the stress changes from the time the gage targets are installed until they are removed. Scratch gages are very convenient for use on bridges since requiring no external data

* Budd Model A-110
** B&F Instruments Model SY 161-100-U

recording equipment, they do not interfere with construction operations or the normal flow of bridge traffic. Also, during the flotation stages of construction of the Rio-Niteroi bridge, when the boxes were completely sealed, other methods of continuous stress measurement were impractical, but the scratch gages, once installed, could be merely left in place for recording stresses during the whole construction sequence. Subsequent to construction, the scratch gages would have recorded any unusual occurrences such as pier settlement, ship impact, large equipment passing over the bridge, etc.

Eight (8) scratch gages were installed in the Rio-Niteroi bridge. Depending on the needs, the location of some gages was changed from one construction stage to another. For example, during the transfer of the north box from the jetties to the pontoon and then to the piers, scratch gages were installed on the outside surface of the top flange at FB27, FB42 and FB51 and later removed and installed inside the box for the stage of the center span lift. Other scratch gages were installed inside the box near the bottom flange and left there.

In the completed structure, the scratch gages are located at FB17, FB27, FB42, FB57 and FB87 (middle of the center span), all inside the box. The position on the web, close to but not on the flanges, was dictated by convenience of installation, and a need to keep the gages from condensation water (or

during construction, rain) which might accumulate at the bottom and from excessive vibration of the top flange due to traffic. The final position of each gage is listed in Fig. 4.

In subsequent text, scratch gages are identified by their location in the structure. For example FB27T means at floor beam 27 at the top of the web and FB27B at the bottom.

Since the initial installation in October 1973, the gages have recorded construction stress changes, test load stress changes, and thermal stress changes. A full summary of all scratch gage records (traces) is contained in Table 2. This table lists the period covered by each scratch gage target, its location in the bridge, and the type of trace obtained.

A scratch gage can be described as a steel strap having one end fixed to the structure surface under it, and the other free end bearing a brass ring on which a scratch is made by a sharp point attached to the surface when the structure deforms due to stress or temperature changes. Since the strap is made of steel similar to the bridge members, the scratch gages are temperature compensating and record only the strains caused by the stress produced by temperature or loads.

As shown in Fig. 5a (here only the portion to the right of the "riveted connection" is discussed , two base plates,

one large A and one small B support other components of the scratch gage mechanism. There are two bundles of thin steel wires, one long C, and one short D, and a scribe point E at the end of the scribe arm F. The right end of the long wire bundle C and the right end of the scribe arm F are mounted on the small base plate. The right end of the short wire bundle D is attached to the large base plate. Two small rollers G on the large base plate hold the left edge of the target H while allowing it to rotate. The target is a circular polished brass ring, 23.6 mm in diameter. The ends of the two wire bundles rest obliquely (pointing counterclockwise) in the peripheral groove of the target on the right side and press it against the rollers. The scribe point bears down on the face of the target ring.

The small base plate and the extension strap (to which the large base plate is riveted) are attached to the structure to be investigated by "attachment screws". As the structure deforms (undergoes a change in strain) in the direction of the gage, the two base plates move relative to one another. When they move away from each other as a result of tensile deformation, the scribe point scratches an approximately radial trace on the target surface. At the same time the long wire bundle C is retracted and its tip slides back (clockwise) in the target groove while the tendency of the target to rotate along with the bundle tip is prevented by the short wire bundle D.

When the base plates move toward each other due to a compressive deformation, the scribe point moves radially on the target surface, but the target in this case does not remain stationary -- it rotates counterclockwise -- being pushed by the tip of the long wire bundle. The short bundle in this case does not resist rotation. The result is that the scratched trace on the target surface is at an angle of 45° with respect to the target radius.

When another tensile deformation is imposed, and the gage bases move apart, another radial scratch is recorded resulting in a continuous zig-zag trace.

The distance between the attachment screws is the gage length. It is divided into the length of the scratch in computing the strains. However, to improve the sensitivity, the gage length is usually increased by attaching the left end of the large base plate A to a steel strap whose far end is then connected to the structure as shown in Fig. 5.

The scratch gages installed in the bridge originally (October and December 1973), had a gage length of 30.5 cm (Fig. 5a). This was an optimum gage length for the expected construction stress changes of the order of 245 MPa (2500 kg/cm^2). Stress changes in the completed bridge were much smaller - 0 to 51 MPa (0 to 525 kg/cm^2) - and it was desirable to increase

the gage sensitivity. This was accomplished in January 1975 by bolting additional extension straps to the original ones. In this manner, all gage lengths were increased to 100 cm (Fig. 5b), with the exception of FB57T, where the length could only be increased to 90 cm due to an obstruction. A supporting screw placed under the straps at midpoint prevented flapping of the long extension straps.

The scratch zig-zag traces made by the gage on the targets vary from approximately 0.025 mm to 0.25 mm in amplitude. Obviously, they can only be measured using some form of magnification. Also, some method of permanently recording the traces is necessary. An optical microscope system was tried, but it proved unsatisfactory. However a scanning electron microscope (SEM) gave excellent results. The advantages of the SEM are as follows: (1) a large observation area for scanning the target to aid in finding the scribe marks, (2) good depth of high resolution field which made it easier to determine where on the target the scribe may have made several passes caused by several stress changes occurring without advancement of the target, (3) a magnification variable to any power, and (4) a permanently affixed polaroid camera.

Analysis of the scratch gage traces was made from the photographs. A trace, like a typical one shown in Fig. 6, goes from left to right and each vertical "zig" (radial on the target) indicates a tensile stress change while a slanted "zag" going up to the right indicates a compressive stress change. The stress change for a particular "zig" or "zag" is computed from

$$\Delta\sigma = \frac{AE}{GM} \tag{2.1}$$

where $\Delta\sigma$= stress change

A = vertical (radial) amplitude of the "zig" or "zag"

E = modulus of elasticity of steel ($E = 2.1 \times 10^6$ kg/cm^2 = 2.06×10^5 MPa)

G = gage length

M = magnification factor of the photograph

Two considerations must be kept in mind when analyzing the record on the scratch gage target. Although the target contains a complete stress history for the period from target installation to removal, the initial stress condition of the member at the time of target installation, although not known, serves as the "zero" stress condition of the scribe point on the target. Secondly, stress changes below a certain level will not result in target advancement (rotation) due to a slight slack in the long wire bundle (driver bundle). As a result, the radial back and forth motion of the scribe point will produce a small polished area until a compressive stress change greater than this

critical level forces the target to rotate. According to literature (1)., the critical stress level should be 29 MPa (300 kg/cm^2) for the 30.5 cm gage length and 9.8 MPa (100 kg/cm^2) for the 100 cm gage length. Some gages, however, have proven to be substantially more sensitive.

A sample stress change computation is shown in Fig. 6. The trace is a record of the construction stress changes in the north box at FB42B. During the transfer of the girder from the jetties to the pontoon, FB42B underwent a compressive stress change causing the scratch gage scribe to move from a position at the bottom left hand side of the photograph to the top center position. The radial (perpendicular to the circumferential groove lines on the target) distance between the two points is 7.1 cm. With the magnification factor of 215 and the gage length of 30.5 cm, Eq. 2.1 yields a stress change of 221 MPa (2250 kg/cm^2). A similar procedure was followed in computing all stress changes recorded on the scratch gage targets.

2.5 Mechanical Gage System

The mechanical gage system is a system of data acquisition in which the distance between two target holes predrilled at a series of locations in the bridge girder is measured by means of a special gage (mechanical gage). The

difference between two readings taken at a particular location divided by the original distance between the two target holes gives the strain change produced by the change in loading between these readings.

The mechanical gage system does not provide a continuous recording of strain changes as do the scratch gages. However, the readings are more accurate and the target holes require less maintenance. Also, only one gage is used for readings at many locations whereas a separate scratch gage is needed for each location. The advantage of the mechanical gage system over the electric gage system is that no external data recording equipment is required and that the readings from different time periods can be dirctly compared for establishing a stress history.

Mechanical gage readings were taken at all instrumented sections (except FB87) on both the north and south boxes at the locations indicated in Figs. 7 and 8. Stresses and strains computed from these readings are listed in Table 3. A total of ten sets were made covering the three stages of construction and several times after completion.

The mechanical gage consists of two conical points connected to a leverage mechanism which transmits the relative

motion between the points to a dial gage for measurement.* As shown schematically in Fig. 9a, the points are inserted into the holes predrilled in the structure. The holes were drilled using special drill bits which made a beveled shoulder on each hole perimeter so that the line of contact would not be susceptible to damage. (See the detail of Fig. 9a.) The holes were also filled with grease and covered with adhesive tape to inhibit rusting during the intervals between readings.

At fifteen of the locations, temperature compensating bars (Fig. 9b) were attached with Epoxy cement in close vicinity of the gage holes. Asterisks in Table 3 indicate the location where compensating bars were read). The difference of strains in the structure and in the compensating bars gives the strain which produces stresses.

To take measurements, the end points of the two bar extensions were fitted into the holes. The points are beveled more sharply than the beveled shoulders, thus they contact the shoulders only on a circular plane (Fig. 9b). After the dial gage was read and the reading recorded by hand, the gage was taken out, turned around and the procedure repeated. This was

---

*The mechanical gage used was of Marion Co. manufacture with the gage length of 20 cm.

repeated once more so that three readings were taken at each location.

An Invar bar is provided with the mechanical gage. The bar does not change length with temperature changes, and was measured several times during each set of readings, providing a correction factor for any change in the dial gage setting.

The data reduction procedure for mechanical gage readings at a particular location is summarized by the following formulas; the first equation giving the change in strain where temperature compensating bars were read:

$$\Delta\varepsilon_{i,i+1} = \frac{1}{G}\{(R_{i+1} - CB_{i+1}) - (R_i - CB_i)\} \qquad (2.2)$$

At locations where temperature compensating bars were not read, the following equation was used:

$$\Delta\varepsilon_{i,i+1} = \frac{1}{G}\{(R_{i+1} - IR_{i+1}) - (R_i - IR_i)\} \qquad (2.3)$$

where:

R_i = Avg. reading between gage holes on the structure for i-th reading period.

CB_i = Avg. reading between gage holes on the compensating bar for the i-th reading period.

IR_i = Avg. reading between gage holes on the Invar bar for the i-th reading period.

R_{i+1}, CB_{i+1}, IR_{i+1} are the respective average readings for the (I+1)th reading period.

G = gage length (20 cm)

An alternative equation can be used to compute strain change produced only by stress change:

$$\Delta\varepsilon_{i,i+1} = \frac{1}{G}\{(R_{i+1} - IR_{i+1}) - (R_i - IR_i)\} - \alpha_T(T_{i+1} - T_i) \quad (2.4)$$

where T_{i+1} = temperature at the (i+1)th reading period and T_i = temperature at the i-th reading period.

3. STRESS, STRAIN AND TEMPERATURE HISTORY

3.1 Introduction

Stress and strain change* measurements were taken at various times at various locations on the bridge. Three measurement records are discussed in this chapter: 1) the record of construction stress changes, 2) the record of test loading stress changes, 3) the record of thermal stress changes. All results are compared to analytically computed values and design values.

The construction phase produced the largest stress changes - up to 245 MPa (2500 kg/cm^2) - five times greater than any other stress changes. The test loadings produced small stress changes - less than 28 MPa (280 kg/cm^2) - and asymmetrical loading distribution between the boxes. Thermal effects produced apparent stress changes of up to 52 MPa (525 kg/cm^2) and indicated that stress changes of up to 98 MPa (1000 kg/cm^2) could be produced at other locations.

---

*"stress change" or "strain change" refers to the change in stress or strain conditions, not the existing condition. A member may undergo a compressive stress change, but still be in a tensile stress condition.

3.2 Construction Stress Changes and Neutral Axis Adjustment

The construction phase resulted in three major stress changes on each of the four half-width side span units (see Fig. 11), the construction sequence being similar for all four units. The first major stress change was during the transferral of the units from the jetties to the pontoon. The support points of the units were changed (Fig. 10) from FB17 + 8 meters and FB57 (192-meter span) to FB27 + 7.5 meters and FB51 - 2.5 meters (110-meter span). Major stress changes were recorded at FB27, FB42 and FB51 (Fig. 12, 13 and 14). The stress changes were tensile at the top flanges and compressive at the bottom flanges (the stress changes were recorded 1-2 cm from the extreme fibers of the flanges). The highest tensile stress changes were recorded at FB27T, the average value (all gage systems) being +193 MPa (+1965 kg/cm^2). The highest compressive stress changes were recorded at FB27B, the average value (all gage systems) being -205 MPa (-2090 kg/cm^2). These values are within 4% of the design values of +187 MPa (+1907 kg/cm^2) and -212 MPa (-2164 kg/cm^2). The average values computed from each individual gage system are in Tables 4 & 5.

The second major stress changes occurred when the units were transferred from the center span pontoon to the piers. The support points were changed (Fig. 10) from FB27 + 7.5 meters and

FB51 - 2.5 meters to FB17 and FB57 (200-meter span). This was recorded at FB27, FB42 and FB51 (Figs. 15, 16, 17); the stress changes being compressive at the top flanges and tensile at the bottom flanges. The highest stress changes recorded were at FB42, the average values being as follows: top flange -173 MPa (-1760 kg/cm^2); bottom flange +235 MPa (+2400 kg/cm^2). These values are within 4% of the design values of -172 MPa (-1754 kg/cm^2) and +244 MPa (+2482 kg/cm^2). The average values computed from each individual gage system are in Tables 4 & 5.

3.2.1 Section Property Adjustment

Moment changes computed from top flange and bottom flange stress changes using the design section properties ($\Delta M = \Delta\sigma \cdot S_{DES.}$) were not identical at each floor beam location for each construction sequence. For example, the moment change computed (for the jetties - pontoon transferral) from the top flange stress change was 274,000 kN-m (30,800 t-m), while the moment change computed from the bottom flange stress change was 262,000 kN-m (29,400 t-m), a ratio of 1.05. This indicated that the location of the neutral axis was somewhat at variance with the location used in design.

All stress changes for the first two construction sequences from strain gage and mechanical gage data are tabulated in Table 4. (Top flange stress changes are

plotted in Figs. 14 and 17.) From each sequence of readings, the ratio of top to bottom stress changes was computed. These ratios were used to compute adjusted C_T (distance from the neutral axis to the extreme top fiber) and C_B (distance from the neutral axis to the extreme bottom fiber) values; ratio = C_T/C_B, depth of section = $C_T + C_B$. Then, the shift of the neutral axis, $\ell = C_{B\ DESIGN} - C_{B\ ADJUSTED}$, and the per cent of shift, $\Delta\ell = \ell/C_B$ were computed. The values are as follows:

	$C_{T\ DES.}$ (cm)	$C_{T\ ADJ.}$ (cm)	$C_{B\ DES.}$ (cm)	$C_{B\ ADJ.}$ (cm)	ℓ (cm)	$\Delta\ell$ (%)
FB27	297.2	304.6	336.6	329.2	7.4	+2.2%
FB42	305.3	308.4	426.2	423.0	3.2	+0.75%
FB51	437.4	457.0	476.6	457.0	19.6	+4.1%

Adjusted C_T and C_B values were not computed for FB17 and FB57 as the stress changes recorded for the first two construction stages were very small.

A check was made on the correctness of the adjusted neutral axis by comparing theoretical stress change values ($\sigma = MC/I$) computed by using adjusted neutral axis values and design moment change values for the jacking of the center span pontoon, with the measured stress change values. The comparison is illustrated in Fig. 18. At FB27 and FB51, the scattering of measured values are grouped around the computed value, but at FB42, the measured stress changes are grouped around a value somewhat smaller than the computed value. It appears that the adjusted neutral axis

is correct, and at FB42, also the moment of inertia is somewhat different than the design value (if the actual moment of inertia were 11% greater than the design value, the measured stress change values would be grouped around the theoretical value). As the shift of the neutral axis is downward, toward the midheight of the bridge, it is on the safe side.

3.3 Construction Moments

The average computed moments (Table 6 & 7) for the three construction sequences are seen in Figs. 19 and 20. The design moment lines supplied by HNTB for the first two construction sequences are plotted in Fig. 19. It is seen that the measured moments are within 4% of design value. At FB51 the measured moment was 412,337 kN-m (46,330 t-m) while the design value was 412,942 kN-m (46,398 t-m) (see Table 8). The discrepancies can be accounted for by errors involved in reading the gages and actual section weights being slightly different than those used in design.** Figure 20 shows the plots of moments computed (Table 7) from the readings taken during the center span lift. The plotted line (which best fits the points) indicates that the pontoon weight was 34,700 kn (3900 tons). The figure

*Howard, Needles, Tammen and Bergendoff, International, Inc.
**See "Section Property Adjustment"

used in design was 3900 tons, with no marine growth on the pontoon. (When the pontoon was lifted, it was seen in fact that very little marine growth had accumulated.)

Due to the close agreement between the measured stress changes and design stress changes (from the moment change diagram), it can be concluded that the design stress values used are accurate; the bridge was not overstressed during construction.

3.4 Parapet and Median Construction

Scratch gage target #8** from FB42B recorded the stress changes caused by the construction of the parapets and median strip. In Fig. 21 a direct correlation is shown between the following: 1) The design stress changes due to the parapet and median construction and the number of days over which the stress changes occurred, 2) The overall stress changes recorded on the target and the number of zigs within each recorded overall stress change. (This correlation confirmed that the zigs were due to stress changes caused by day-night temperature fluctuations in the bridge.* This topic is discussed in detail in section 3.7.

**Table 1

* The computer analysis developed for the bridge which shows that temperature fluctuations could not have been high enough to cause stress changes of the magnitude recorded. This, at present, is unexplainable.

For example, between 15JAN74 and 21JAN74 (7 days), a theoretical stress change of 17 MPa (175 kg/cm^2) was calculated. This corresponds to an overall stress change on the trace of 17 MPa (175 kg/cm^2) occurring over seven zigs.

The establishment of this correlation has two important consequences. Firstly, the date of an occurrence causing an unusually large stress change can be determined. This was done in the case of a violent storm which occurred on 17MAY75. (This is further discussed in section 3.7.1.) Secondly, it aided in establishing the fact that traffic stress changes were very small. From traffic information supplied by ECEX, a periodicity of traffic loading on the bridge was observed. The total number of vehicles crossing the bridge during the week (Monday - Friday) is fairly uniform. During the weekend, the number of cars increases substantially, from 50% to 100% greater than during the week. This periodicity is not reflected on the scratch gage traces (for instance see Fig. 22).

3.5 Test Loading

Prior to the opening of the bridge to traffic a test loading was performed. The test loading operation was subject to three criteria: 1) Production of maximum stresses at FB17, 27, 42, and 57 with the allotted number of 21-17.5 ton trucks; 2)Production

of asymmetrical stress conditions, especially at FB42 which contains no cross bracing; 3) The test loading intensity should nowhere exceed norm loads.*

In order to specify locations for the trucks, a fast method (as time was short) of computing stress changes from different test load patterns was needed. The moment distribution method was used, and influence lines were computed and plotted for moments at FB17, 27, 42, 51 and 57. These influence lines were used to choose four test load positions (see Fig. 23) which satisfied the criteria. (Subsequent to the choosing of the test load schemes, more accurate influence lines were supplied by HNTB,** and these lines were sufficiently close to computed lines so as to require no modification of the test load positions.)

The stress changes caused by the test loads were small and it was doubtful as to whether they would be recorded by the scratch gages. One gage, at FB42B, worked exceptionally well, however. The daily temperature stress changes being recorded ($\approx$50 MPa) at this location were equal to the theoretical stress changes computed for the test loadings. Therefore, while zigs

---

*Brazilian Code

** Howard, Needles, Tammen and Bergendoff, International

caused by the test load stress changes were being recorded on the target it is not possible to clearly distinguish them from the zigs caused by thermal stress changes. It was determined though that the theoretical stress change of 50 MPa was not exceeded.

The electrical strain gages provided the best results of the test loading operation. Two sets of measurements were taken with the test load trucks within the side span, test loads #2 and #4 (Fig. 24). The average stress changes for each set were computed using Simpson's rule for top and bottom flanges, and are as follows:

	Loaded Box	Unloaded Box
Test Position 2:		
Top Flange	9.2 MPa (94 kg/cm^2)	7.4 MPa (75.5 kg/cm^2)
Bottom Flange	24.8 MPa (252 kg/cm^2)	20.6 MPa (210 kg/cm^2)
Test Position 4:		
Top Flange	21.7 MPa (221 kg/cm^2)	18.1 MPa (184 kg/cm^2)
Bottom Flange	18.1 MPa (184 kg/cm^2)	15.3 MPa (156 kg/cm^2)

The average stress distribution was 55% to the loaded box and 45% to the unloaded box. This is equal to the design values of 55% and 45%.

For load position 1, the trucks were positioned in the center span. At FB42 (side span), the ratio of stress distribution was approximately 50% and 50% (not enough gages functioned properly to compute exact values). The trend toward 50-50 stress distribution when the loading is not within the span is proper.

3.6 Temperature Distribution

Figure 25 is a composite of temperature changes recorded on the north and south boxes at FB27 and FB57 on 17Jan75. Each point represents the difference between the temperature at 6:30 (when the bridge temperature was minimum and uniform) and at 15:00 (the time of maximum bridge temperature). The composite was used as a basis for determining the overall temperature change distribution at any bridge cross section.

Since the temperature of the bridge was essentially uniform at 6:30, Figs. 26 and 27 show the temperature change at 15:00. This uneven temperature change induces stresses and strains within each cross section. It can be seen from these that the maximum temperature difference between a structural member exposed to sunlight, and another in the shade is 11.5°C. Since the readings shown were taken on a day (17JAN75) when air temperature reached the highest recorded level (39°C) for one entire year and the day was sunny the figure of 11.5°C can be assumed to be close to, if not the maximum, temperature difference ever occurring in the structure.

In HNTB's preliminary analysis of the structure for thermal effects two temperature distributions were used. One, a maximum temperature differential of 15°C between a top flange

member subjected to the sun's rays, and a shaded flange member, was assumed. It was assumed that this differential varied linearly from the top flange to the bottom flange. Two, a top flange temperature of 15°C with the rest of the structure at 0°C was assumed. These assumptions were shown to be on the safe side as the maximum measured differnential was 11.5°C, the differential dropping off much more quickly toward the bottom flange than HNTB's assumed distribution. For other examples of bridg temperature studies see reference 2.

3.7 Thermal Effects

A continuous record of thermal stress changes from JAN74 to JUN75 has been provided by a sequence of targets from FB42B. The first period of thermal stress change recording began immediately subsequent to the field splice (making the span continuous) on 5JAN74, and ended on 28FEB74 when the target was removed.* A photograph of this trace is in Fig. 22. Forty separate zigs can be counted on the photograph. This number is less than the number of days - 50 - recording time,

* Computations have shown that temperature fluctuations were not sufficiently large to cause stress changes high enough (300 kg/cm^2) to be recorded by the scratch gages prior to the field splice.

but the difference can be accounted for by the two blobbed areas where scribe advancement was prevented for a short period of time (by dirt or some other obstruction). The magnitude of all zigs is approximately the same, and the stress change computed from each zig is 30 MPa (305 kg/cm^2). (The trace on this target also provides a record of stress changes due to the construction of the parapets and medians - see Art. 3.4.) The remainder of the record was recorded on targets #15, #22 and #32 (Table 2).

Figure 28 shows photographs of the portions of two scratch gage traces - from FB27B and from FB42B - where the highest thermal stress changes were recorded (DEC75). The apparent maximum stress change was computed to be 52 MPa (530 kg/cm^2). Since the recording periods extended over one year's time, 52 MPa can be taken as the maximum diurnal stress change, well below the yield stress of the bridge steel. (see footnote on page 29.)

Figure 29 shows a comparison of the thermal stress change zigs recorded by the scratch gages with the different gage lengths (30.5 cm and 100 cm), both from FB42B. The increased gage length increased the size of the daily zigs making for easier analysis.

3.7.1 Scratch Gage Trace Vs. Temperature Data

The most exact correlation between daily air temperature

variations and thermal stress changes was obtained from the scratch gage target (#32) at FB42B which was in place from 17JAN75 to 9JUN75. A photograph of a portion of the target trace covering the period 16MAY75 to 9JUN75 is shown in Fig. 30. Below the photograph is a charted summary of air temperature conditions which prevailed over this period (the summary was prepared from temperature graphs supplied by ECEX). One can observe that larger compressive stress conditions (higher zigs on the trace) correspond to nights when the air temperature was cooler, and higher tensile stress conditions (lower zigs on the trace) correspond to hotter air temperatures during the day. For example, the air temperature on 1 June was higher than the day before or the day after. This is reflected by the zig corresponding to 1 June which shows a larger tensile stress condition than the two zigs on either side. The heavier arrow indicates the area on the trace where a number of smaller stress changes - 10-12 MPa (100-120 kg/cm^2) - took place. This area corresponds to the time - 16:00 hrs, 17MAY75 - when a violent storm with heavy winds occurred.

Thus it is possible to match specific zigs on the target with the days on which they were recorded. Future events causing large stress changes (e.g. an extremely heavy load crossing the bridge) can be pinpointed as to which day they occurred.

4. CONCLUSIONS

The following conclusions can be drawn from this study:

1) Observed stress changes during construction were close to the figures used for design - the bridge was not overstressed during construction. The method of analysis used in design was proven accurate.

2) The distribution of one-sided loading between the boxes of 55% to the loaded box and 45% to the unloaded box for the loaded girders was confirmed.

3) The measured temperature distribution through the cross section was different than the distribution assumed for design, However, the temperature distribution assumed for design would produce higher stress changes than the measured distribution. The measured temperature distribution may be used in the design of similar structures.

4) A good correlation was found between measurements from the different instrumentation systems for the construction stress changes.

5) The scratch gage was proven to be a reliable device for measuring stress changes.

6) The scratch gages on the bridge are recommended for monitoring future stress changes.

TRIP	READING NUMBER	DATE	START TIME	DESCRIPTION
1	1	17Jul73		No readings during this trip
2	2	03Sep73		No readings (Installation of Instrumentation)
3	3.0	080ct73	16:10	Side span on jetties
	3.1	090ct73	13:00	Side span on jetties
	3.2	100ct73	00:20	Side span on pontoon
	3.3	110ct73	22:25	Side span on pontoon
	3.4	120ct73	05:50	Side span on pier rings
4	4.0	12Dec73	00:36	Pontoon in water
	4.1	13Dec73	09:30	Pontoon suspended (day)
	4.2	13Dec73	20:40	Pontoon suspended (night)
5	5.0	25Feb74	06:45	Zero readings - test loads
	5.1	24Feb74	22:52	Load position 1
	5.2	25Feb74	03:25	Load position 2
	5.3	25Feb74	20:36	Zero reading - test loads
	5.4	25Feb74	23:58	Load position 3
	5.5	26Feb74	02:35	Load position 4
	5.6	26Feb74	14:15	Temperature study
	5.7	27Feb74	11:05	Temperature study
6	6.1	10Jun74	08:56	Temperature study
	6.2	11Jun74	07:50	Temperature study
7	7.1	16Jan75	23:00	Temperature study

Table 1 Sequence of Electrical Gage Static Readings

No.	STATION (Longitud. Location)	PERIOD From - To	PATTERN		COMMENTS
1	2	3	4	5	6
1	FB27 -Bot.	OCT73 -14DEC73		**	Good record: Jetties-pontoon-piers-pontoon lift
2	FB27 -Top	OCT73 -02DEC73		**	Good record: Jetties-pontoon-piers
3	FB42 -Top (outside)	OCT73 -02DEC73		**	Good record: Jetties-pontoon-piers (Gage may have been jarred causing scratch irregularity)
4	FB17 -Top	14DEC73 -28FEB74			No scratch on target, only some dots
5	FB17 -Bot.	14DEC73 -28FEB74			No scratch on target
6	FB27 -Bot.	14DEC73 -28FEB74		*	Faint blob
7	FB42 -Top	OCT73 -28FEB74		**	Good record: Jetties-pontoon-pier-pontoon lift
8	FB42 -Bot.	OCT73 -28FEB74		**	Good record: Jetties-pontoon-pier-pontoon lift-parapet placement-test loads (also recorded daily thermal stress changes)
9	FB57 -Top	14DEC73 -28FEB74		*	Line of small scratch marks recorded on target-apparently the result of daily thermal stress changes

* - Approximate magnification = 50
** - Approximate magnification = 300

TABLE 2 SCRATCH GAGE TARGETS

No.	STATION (Longitud. Location)	PERIOD From - To	PATTERN		COMMENTS
1	2	3	4	5	6
10	FB57 -Bot.	14DEC73 -28FEB74		*	Target advancement and compressive scratch recorded, but angle appears too flat and scratch may have resulted from a jarring of the gage
11	FB8Z-Top (Center span)	22FEB74 -28FEB74			No scratch on target
12	FB17 -Top	28FEB74 -06JUN74			No scratch on target
13	FB27 -Bot.	28FEB74 -06JUN74		**	No scratch, only some blobs
14	FB42 -Top	28FEB74 -06JUN74		**	Scratch probably a result of other than bridge stress changes (possibly a jarring of the target)
15	FB42 -Bot.	28FEB74 -06JUN74	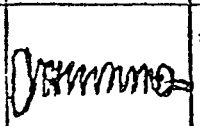	**	Good results: thermal stress changes subsequent to test loadings
16	FB57 -Top	28FEB74 -06JUN74			No scratch on target
17	FB57 -Bot.	28FEB74 -06JUN74		**	Small blob - no target advancement
18	FB87 -Top	28FEB74 -06JUN74		**	Small blob - no target advancement

* - Approximate magnification = 50
** - Approximate magnification - 300

TABLE 2 (Cont'd) SCRATCH GAGE TARGETS

	STATION (Longitud. Location)	PERIOD From - To	PATTERN		COMMENTS
1	2	3	4	5	6
19	FB17 -Top	6JUN74 -10JAN75			No scratch on target
20	FB27 -Bot	6JUN74 -10JAN75	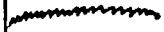	*	Good record: Daily thermal stress changes. Approximately 80 separate zigs
21	FB42 -Top	6JUN74 -10JAN75		*	Weak trace
22	FB42 -Bot	6JUN74 -9JAN75	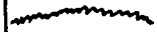	*	Good record: Daily thermal stress changes. Approximately 130 separate zigs.
23	FB42 -Bot	11JAN75 -15JAN75		**	Good record: 5 thermal stress changes recorded. (Gage extension in place)
24	FB57 -Top	6JUN74 -9JAN75		**	16 separate zigs. Gage appears to have operated properly for only 2 weeks.
25	FB57 -Bot	6JUN74 -8JAN75			No scratch on target
26	FB57 -Bot	10JAN75 -14JAN75		**	Jumble of scratches. (Gage extension in place)
27	FB87 -Top	6JUN74 -11JAN75		**	Small scratch. No target advancement

* - Approximate magnification = 50
** - Approximate magnification = 200

TABLE 2 (Con'd) SCRATCH GAGE TARGETS

No.	STATION (Long. Location	PERIOD From -To	PATTERN		COMMENTS
1	2	3	4	5	6
28	FB17 -Bot	15JAN75 -19JUN75		*	Daily thermal stress changes recorded, but slow target advance-ment
29	FB27 -Top	17JAN75 -9JUN75	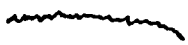	*	Daily thermal stress changes recorded
30	FB27 -Bot	15JAN75 -19JUN75	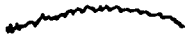	*	Daily thermal stress changes recorded, but target surface is corroded
31	FB42 -Top	15JAN75 -9Jun75			No scratch on target
32	FB42 -Bot	16JAN75 -9JUN75	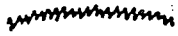	*	Good record: Daily thermal stress changes
33	FB57 -Top	15JAN75 -9Jun75			One blob, no advancement
34	FB57 -Bot	15JAN75 -9JUN75		**	Irregular trace, scribe slipped off
35	FB87 -Bot	16JAN75 -19JUN75		**	Series of blobs (Target corroded)

* - Approximate Magnification = 50
** - Approximate Magnification = 200
NOTE: Gage Extensions in Place at all Locations.

TABLE 2 (Cont'd) SCRATCH GAGE TARGETS

LOCATION	GAGE	JETTIES TO PONTOON (SOUTH)	PONTOON TO PIERS (NORTH)	CENTER SPAN LIFT (NORTH)	ON JETTIES TO BRIDGE COMPLETION (SOUTH)	JAN75-JUN75 (NORTH)*
1	2	3	4	5	6	7
FB17 TOP	1		-26.7			
	3		-73.9			
	5		-51.3			
	1a			- 140.6		
	3a			- 63.3		-200*
	5a			- 118.0		
	6	- 105				
	7	- 262				
	8	- 105				
FB17 BOTT.	1b					-195*
	2b					
	3b					-200*
	4b					
	5b					-188*
	6b				+ 897	
	7b					
	8b				+1421	
FB27 TOP	9		-2101			
	11		-2208			
	13		-2347			
	9a			+ 892.8		-195*
	11a			+ 970.1		
	13a			+1040.4		-163*
	14	+1890				
	15	+1995				
	16	+1995				
	14a					
	15a					
	16a					
FB27 BOTT.	9b					
	10b					
	11b			- 984.2		
	12b			- 871.7		
	13b			-1377.9		
	14b				+ 704	
	15b				+ 599	
	16b				+ 939	

*Strain Changes (10^{-6} cm/cm)

Table 3 Stress Changes (kg/cm^2) - Mechanical Gage Readings

LOCATION	GAGE	JETTIES TO PONTOON (SOUTH)	PONTOON TO PIERS (NORTH)	CENTER SPAN LIFT (NORTH)	ON JETTIES TO BRIDGE COMPLETION (SOUTH)	JAN75-JUN75 (NORTH)*
1	2	3	4	5	6	7
	17		-1691			
	18		-1779			
	19		-1916			
	17a			+1321.6		-263*
FB17 TOP	18a			-3859.6		
	19a			+1251.3		-200*
	20	+1732				
	21	+1785				
	20a					
	21a					
	17b			-1659.1		
FB42 BOTT.	18b			-1982.5		
	19b			-1926.2		
	20b				+2293	
	21b				+1596	
	22		-2031			
	24		- 511			
	26		-1034			
FB51 TOP	22a			+ 864.7		
	24a			+1054.5		
	26a			+1068.8		-170*
	27	+ 892				
	28	+1102				
	28a					
	22b			-1160.0		
FB51 BOT	23b			-1138.9		
	24b			-1181.0		
	25b			-1448.2		
	26b					-250*
	28b				+1533	

*Strain Changes (10^{-6} cm/cm)

Table 3 (Cont'd) Stress Changes (kg/cm^2) - Mech. Gage Readings

LOCATION	GAGE	JETTIES TO PONTOON (SOUTH)	PONTOON TO PIERS (NORTH)	CENTER SPAN LIFT (NORTH)	ON JETTIES TO BRIDGE COMPLETION (SOUTH)	JAN75-JUN75 (NORTH)*
1	2	3	4	5	6	7
	29					
	31		-144			
	33		-129			
	29a			+688.9		-200*
	30a			+822.5		
	31a			+921.0		-225*
FB57 TOP	32a			+745.2		
	33a			+820.0		-225*
	34					
	35	÷ 52				
	36	÷262				
	34a					
	35a					
	36a					
	29b			-921.0		
	30b			-829.5		
	31b					
FB57 BOTT.	32b			-836.6		
	33b			-829.5		
	34b				+ 851	
	35b					
	36b				+1481	

*Strain Changes (10^{-6} cm/cm)

Table 3 (Cont'd) Stress Changes (kg/cm^2) - Mech. Gage Readings

1) FB27

1.1) Jetties to Pontoon

Top Flange

Strain [1920 + 1939(2) + 2003]/4 = 1950
Mech [1890 +1995(2) + 1995]/4 = 1970 } 1960

Botton Flange

Strain [2222 + 2081 + 2191 + 2089 + 2121 + 2040]/7 = 2120

1960/2120 = 0.925

1.2) Pontoon to Piers

Top Flange

Strain [2215 + 2209 + 2300]/3 = 2240
Mech [2101 + 2208(2) + 2247]/4 = 2220 } 2230

Bottom Flange

Strain [2358 + 2355 + 2425 + 2504]/4 = 2410

2230/2410 = 0.925

$C_T/C_B = 0.925$; $C_T + C_B = 634.7\text{cm} = d_{Des.}$

$C_T = 305.0$ cm

2) FB42

2.1) Jetties to Pontoon

Top Flange

Strain [1740 + 1799(2) + 1705]/4 = 1760
Mech [1734 + 1785]/2 = 1760 } 1760

Botton Flange

Strain [2427 + 2427 + 2326 + 2326]/4 = 2380

1760/2380 = 0.739

2.2) Pontoon to Piers

Top Flange

Strain [1797 + 1835(2) + 1780]/4 = 1810
Mech [1691 + 1779(2) + 1916]/4 = 1790 } 1800

Table 4 Stress Changes (kg/cm^2) Jetties to Pontoon - Pontoon to Piers and Effective Location of N.A.

Bottom Flange

Strain [2436 + 2467 (2) + 2564] /4 = 2484

1800/2484 = 0.725

[.725+ .739]½ = .732 = C_T/C_B; $C_T + C_B$ = 731.1cm = $d_{Des.}$

C_T = 309.0 cm

3) FB51

3.1) Jetties to Pontoon

Top Flange

Strain [1094 + 1100(2) + 1089]/4 = 1095
Mech [892 + 1102]/2 = 1000
} 1047.5

Bottom Flange

Strain [1044 + 1029 + 1064]/3 = 1040

1047.5/1040 = 1.0072

3.2) Pontoon to Piers

Top Flange

Strain [1096 + 1069(2) + 1096]/4 = 1080
Mech [990 + 1034]/2 = 1010
} 1045

Bottom Flange

Strain [1037 + 1034 + 1075]/3 = 1050

1045/1050 = .9952

[1.0072 + .9952]/2 = 1.00 = C_T/C_B

$C_T + C_B$ = 918.8 cm = $d_{Des.}$

$C_T = C_T$ = 459.4 cm

Table 4 (Cont'd) Stress Changes (kg/cm^2) Jetties to Pontoon – Pontoon to Piers

	CONSTRUCTION SEQUENCE	STRESS CHANGE (kg/cm^2)	$\frac{C_{FL.}}{Y_{S.G.}}$	EXTRAPOLATED STRESS CHANGE IN FLANGE (kg/cm^2)
1	2	3	4	5 = 3 x 4
FB27 TOP	Jetties - Pontoon	1970	1.095	2156
	Pontoon - Piers	2210	1.095	2418
FB27 BOTT	Jetties - Pontoon	2060	1.065	2198
	Pontoon - Piers	2210	1.065	2351
	Center Span Lift	820	1.065	869
FB42 TOP	Jetties - Pontoon	1680	1.053	1768
	Pontoon - Piers	1680	1.053	1768
	Center Span Lift	1440	1.053	1516
FB42 BOTT	Jetties - Pontoon	2250	1.066	2405
	Pontoon - Piers	2300	1.066	2456
	Center Span Lift	1730	1.066	1846

$$\frac{C_{FL.}}{Y_{S.G.}} = \frac{\text{Distance from centroid to extreme fiber of flange}}{\text{Distance from centroid to scratch gage}}$$

Table 5 Stress Changes from Scratch Gage Targets - Construction Stages

LOCATION		JETTIES - PONTOON	PONTOON - PIERS
Top FB27	1	(-1960 kg/cm^2)(1.5773 x 10) = -30,915 tm	(2230 kg/cm^2)(15.773) = +35,174 tm
BOTT	2	(-2120 kg/cm^2)(1.4595 x 10) = -30,941 tm	(2410 kg/cm^2)(14.595) = +35,174 tm
TOP FB42	3	(-1760 kg/cm^2)(2.5288 x 10) = -44,330 tm	(1800 kg/cm^2)(125.288) = +45,338 tm
BOTT	4	(-2380 kg/cm^2)(1.8437 x 10) = -43,880 tm	(2500 kg/cm^2)(18.437) = +46,090 tm
FB51	5	Avg. ΔM^* = (1045 kg/cm^2)(4.4332 x 10) = 46,330	

*Stress changes for all four cases at FB51 TOP, Jetties-Pontoon, BOTT, Jetties-Pontoon, TOP, Pontoon-Piers, BOTT, Pontoon-Piers, were very close to each other and an average stress change was taken for the moment computation.

Table 6 Computation of Moment Changes - Jetties to Pontoon - Pontoon to Piers (Adjusted Location of Neutral Axis)

LOCATION		MECHANICAL GAGES	STRAIN GAGES
1		2	3
Top FB17	1	(100 kg/cm^2)(1.3832 x 10) = +1,383 tm*	0.0 tm
Bottom	2	NO READINGS	NO READINGS
Top FB27	3	(970 kg/cm^2)(1.5773 x 10) -15,300 tm	(980 kg/cm^2) (15.773) = -15,458 tm
Bottom	4	(1050 kg/cm^2)(1.4595 x 10) = -15,325 tm	(1123 kg/cm^2) (14.595) = -16,390 tm
Top FB42	5	(1290 kg/cm^2)(2.5230 x 10) = -32,493 tm	(1350 kg/cm^2) (25.230) = -34,004 tm
Bottom	6	(1880 kg/cm^2)(1.8468 x 10) = -34,660 tm	(1950 kg/cm^2) (18.468) = -35,950 tm
Top FB51	7	(1050 kg/cm^2)(4.4332 x 10) = -46,549 tm	(1243 kg/cm^2) (44.332) = -55,105 tm
Bottom	8	(1160 kg/cm^2)(4.4332 x 10) = -51,425 tm	(1176 kg/cm^2) (44.332) = -52,134 tm
Top FB57	9	(811 kg/cm^2)(6.7938 x 10) = -55,093 tm	(1212 kg/cm^2) (67.938) = 82,341 tm**
Bottom	10	(848 kg/cm^2)(6.3001 x 10) = -53,425 tm	(1003 kg/cm^2) (63.001) = -63,190 tm

*This moment change apparently corresponds to equivalent temperature change.

**This stress was affected by stress concentrations and system problems.

Table 7 Computation of Moment Changes - Center Span Lift (Adjusted Location of Neutral Axis)

Instrumented Section at Floor Beams					
FB	17	27	42	51	57
x (m)	-0.5	50.5	124.6	170.5	198.9
Column	1	2	3	4	5
$I\ (m^4)$	3.371	4.811	7.796	20.366	42.064
d (cm)	568.3	634.7	731.1	918.8	1286.8
C_T (cm)	243.7	297.3	302.8	439.5	619.2
C_B (cm)	324.6	337.4	428.3	479.3	667.6
$S_T\ (m^3)$	1.3832	1.6180	2.5751	4.6336	6.7938
$S_B\ (m^3)$	1.0385	1.4257	1.8200	4.2498	6.3001
ΔM: J-P	0	-30.855	-45,169	-46,398	-1730
(tm) P-PR	0	+35,146	+47,333	+47,245	+1,762
C.Span Lift	0	-15,079	-37,206	-50,911	-59,392

Notes:

1) Depths, d, were computed by parabolic interpolation between the values at neighboring 10-m stations supplied by the designer (HNTB).

2) Moments of inertia, I, were computed by parabolic interpolation except at FB42 where cross-sectional dimensions were used.

3) Moment changes, ΔM, were computed by linear interpolation from the moment diagrams supplied by the designer (HNTB).

Table 8 Design Values Used in Analysis

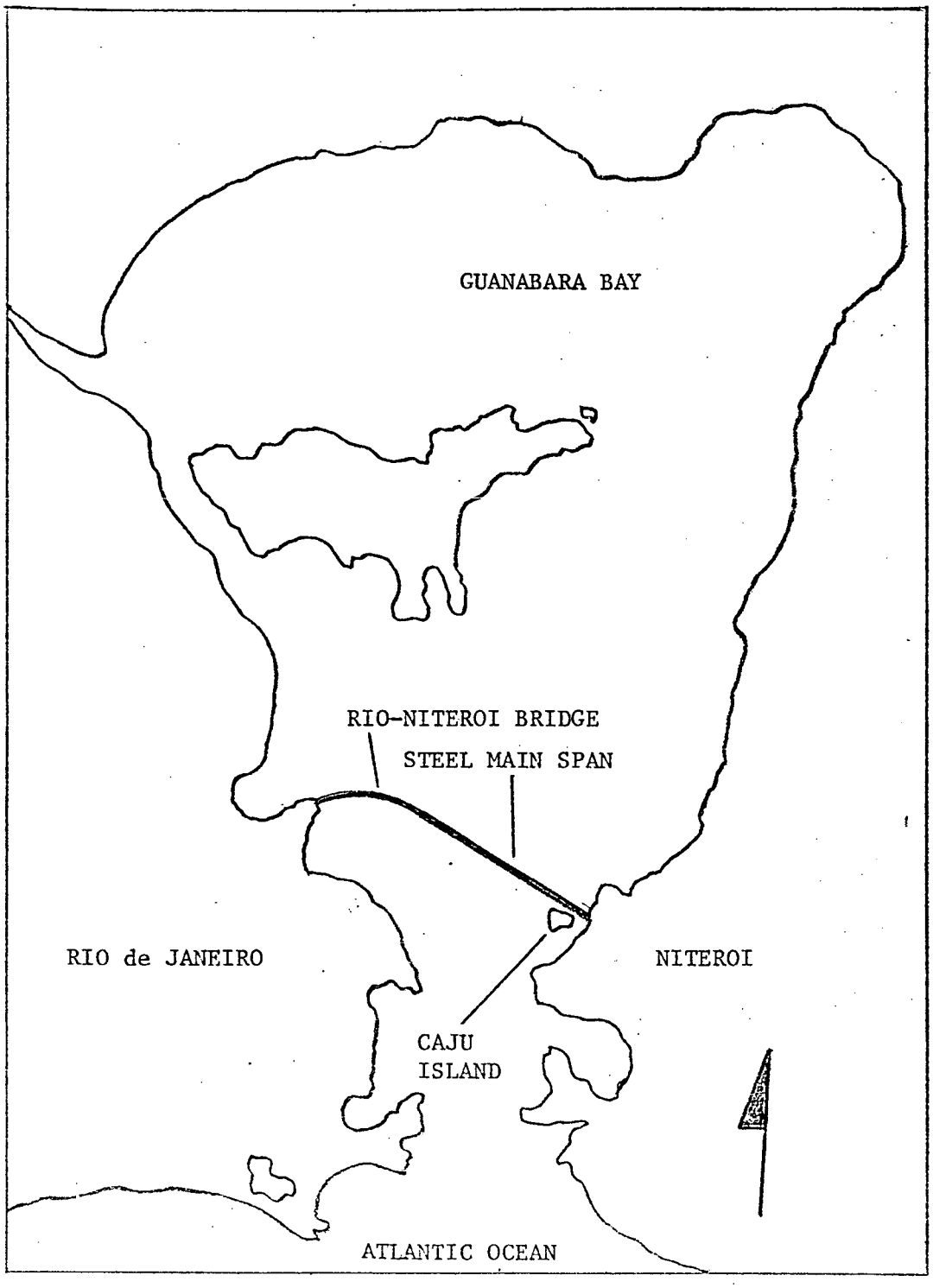

Fig. 1 Rio-Niteroi Bridge Location

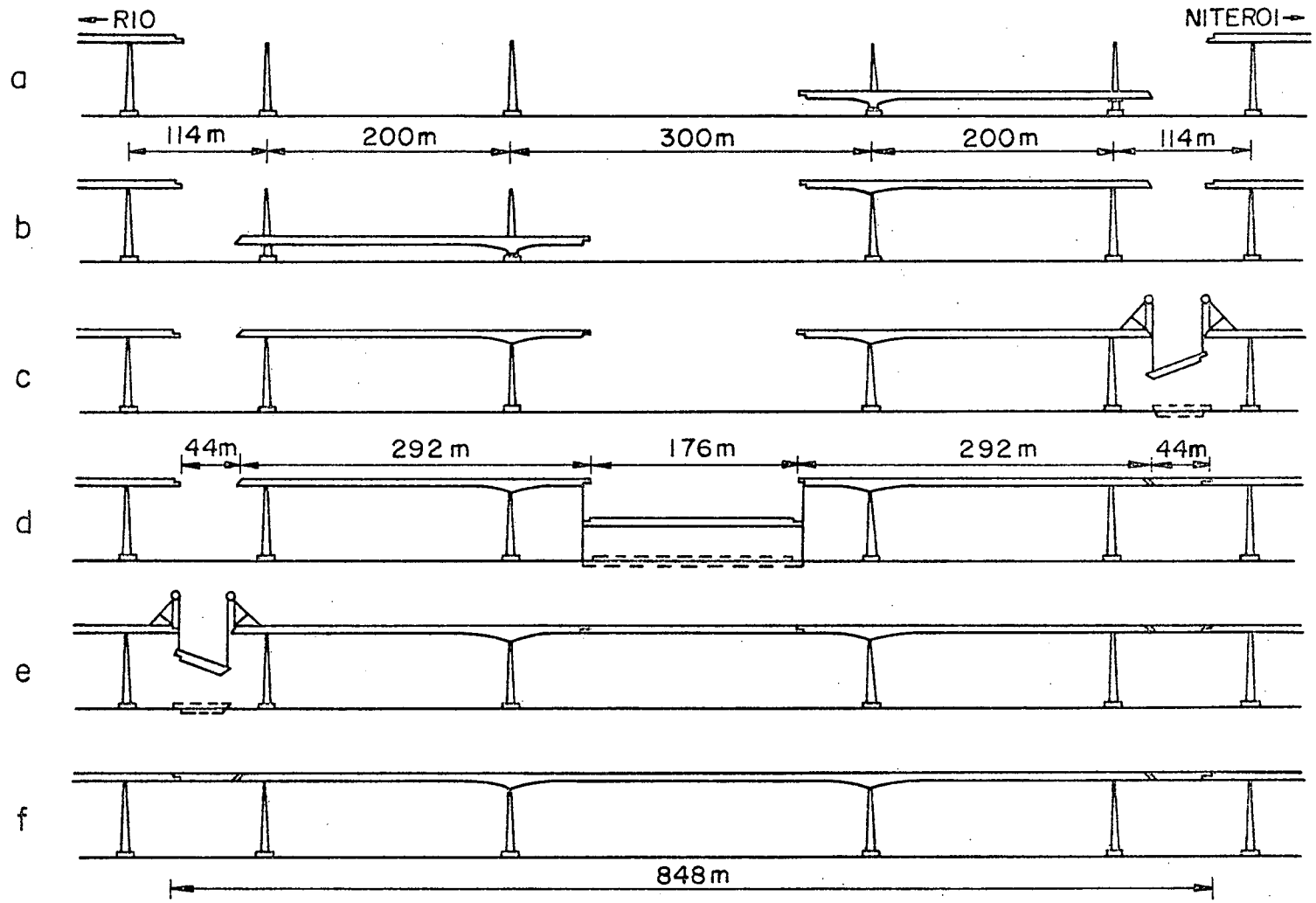

Fig. 2 Steel Erection Sequence

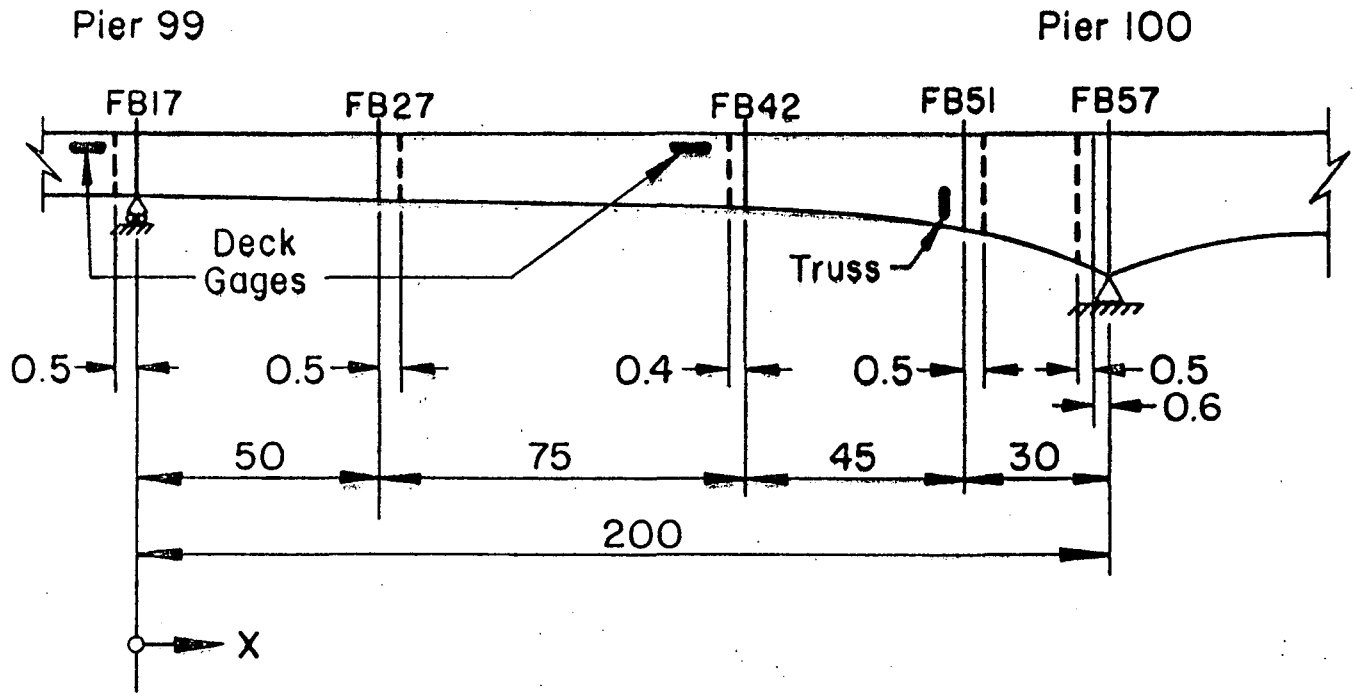

Fig. 3 Location of Instrument Sections

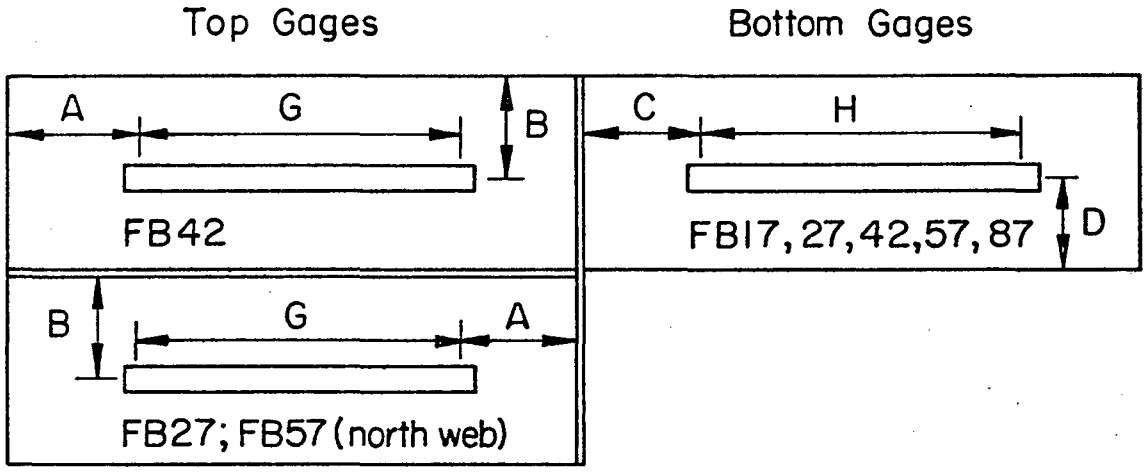

	TOP GAGES			BOTT. GAGES		
	A	B	G	C	D	H
FB17	-	-	-	40.0	32.0	100.0
FB27	25.0	26.5	100.0	23.0	20.0	100.0
FB42	30.0	15.5	100.0	20.0	26.0	100.0
FB57	25.0	31.0	90.0	31.5	20.0	100.0
FB87	-	-	-	21.0	25.0	100.0

All Dimensions In cm.

All gages on south web, except as noted.

A = Distance from attachment screws to floor beam

B = Distance from center of gage to top flange

C = Distance from attachment screws to floor beam

D = Distance from center of gage to bott. flange

G = Gage length

H = Gage length

Fig. 4 Scratch Gage Positions

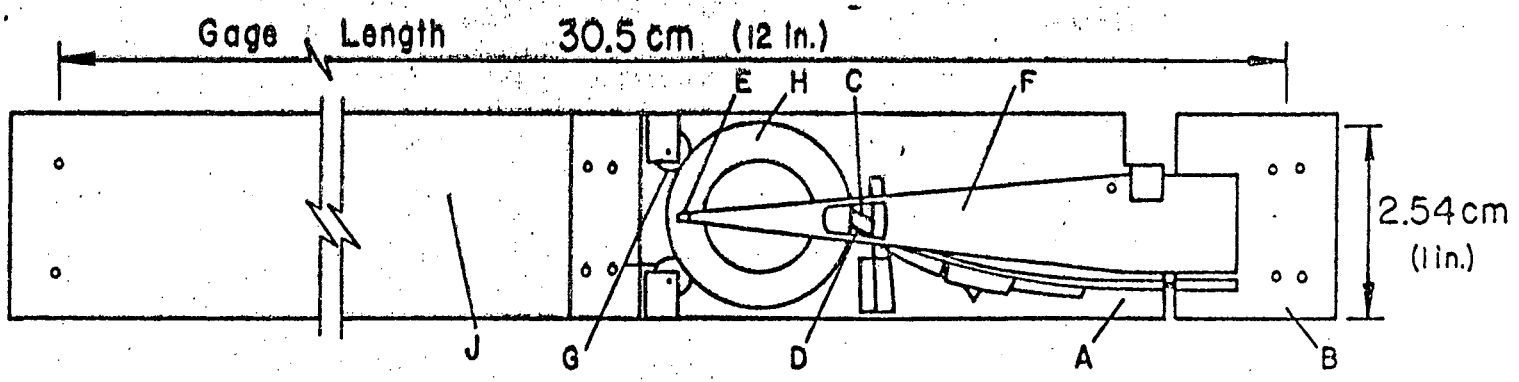

A Large Base Plate
B Small Base Plate
C Driver Brush
D Retainer Brush

(a)

E Scribe Point
F Scribe Arm
G Rollers
H Target
J Extension Strap

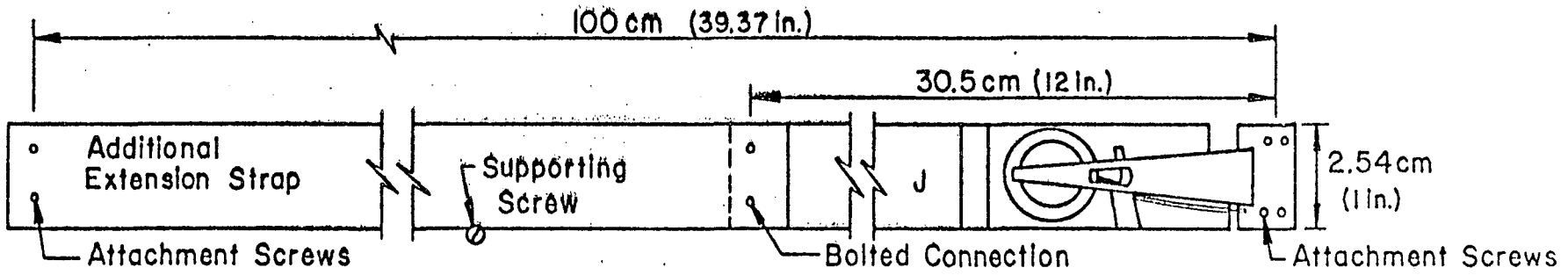

(b)

Fig. 5 Scratch Gage

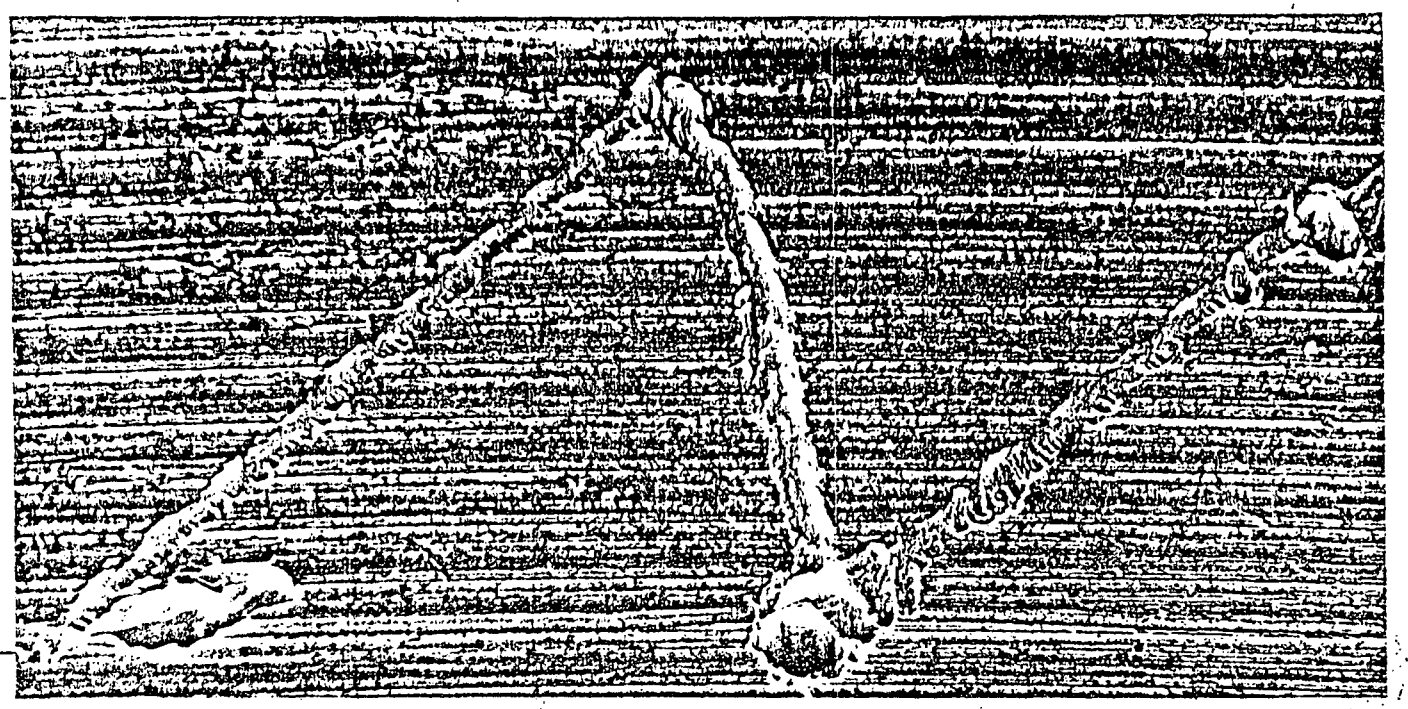

$$\Delta\sigma = \frac{AE}{MG} = \frac{(7.1\ \text{cm})(2.1 \times 10^{6}\ \text{kg/cm}^{2})}{(215)(30.5\ \text{cm})} = 2250\ \text{kg/cm}^{2}$$

FIG. 6 SAMPLE COMPUTATION OF STRESS CHANGE FROM SCRATCH GAGE TRACE

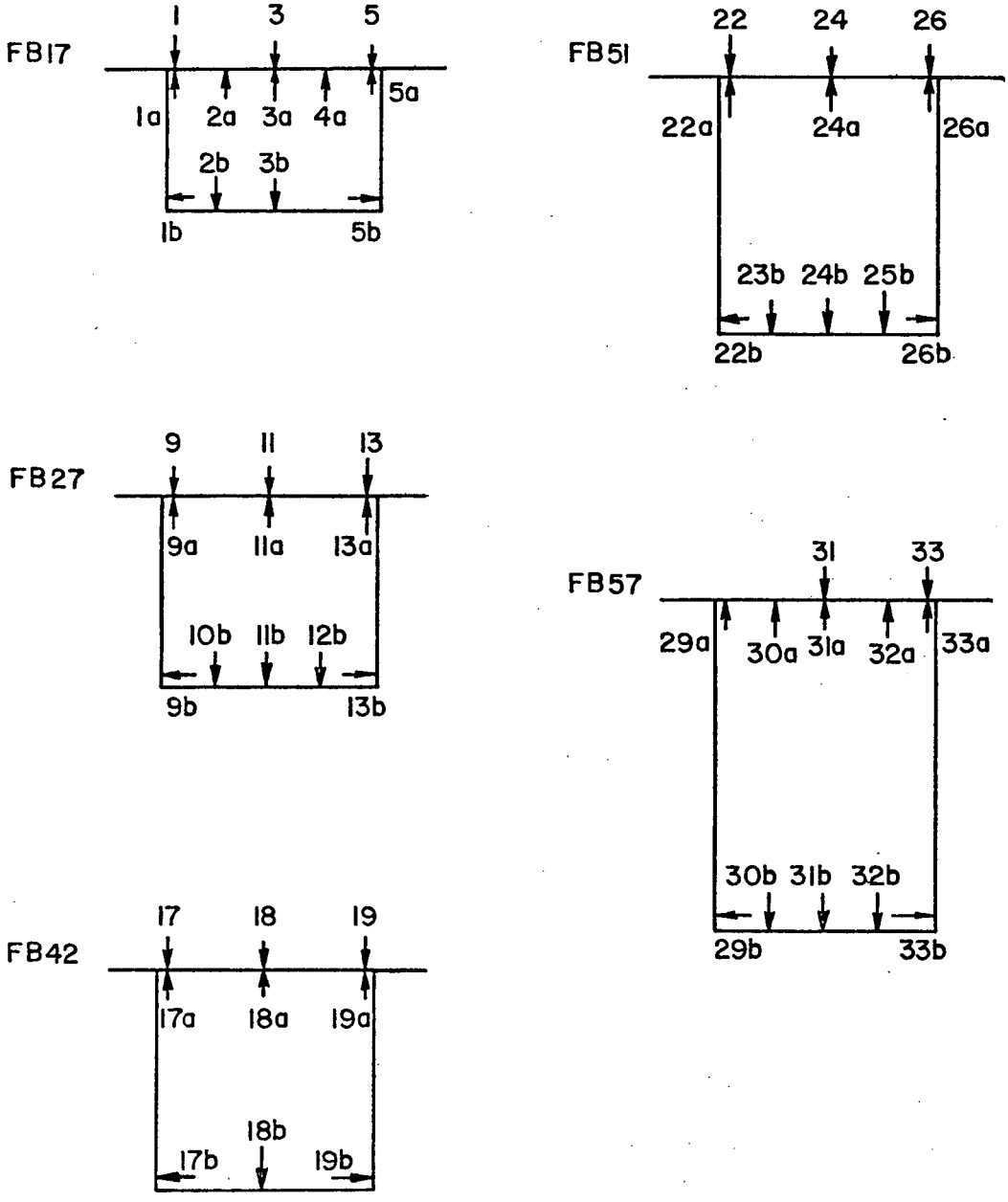

Fig. 7 Mechanical Gage Hole Locations (North Box)
(View toward Niteroi)

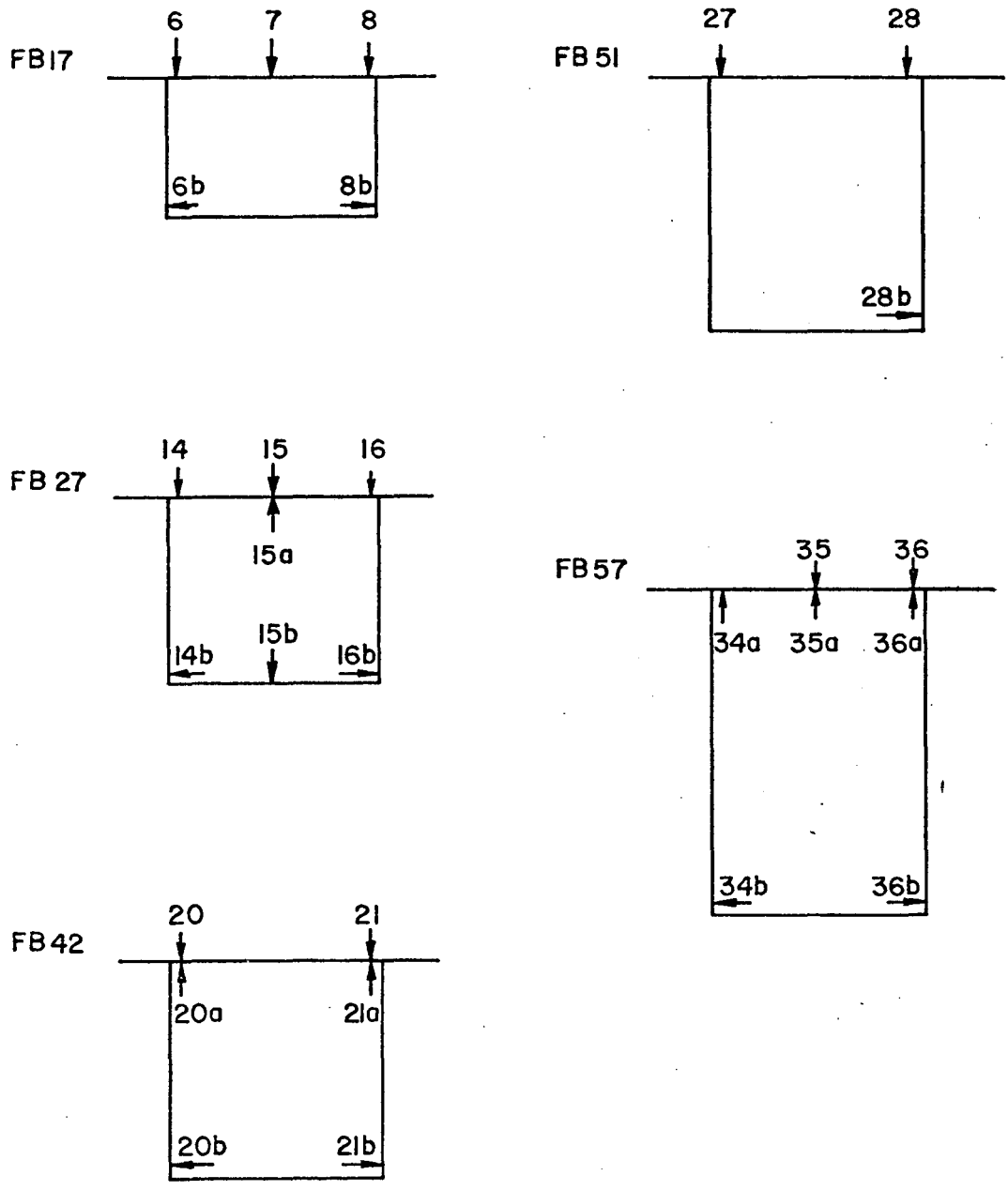

FIG. 8 Mechanical Gage Hole Locations (South Box)
(View toward Niteroi)

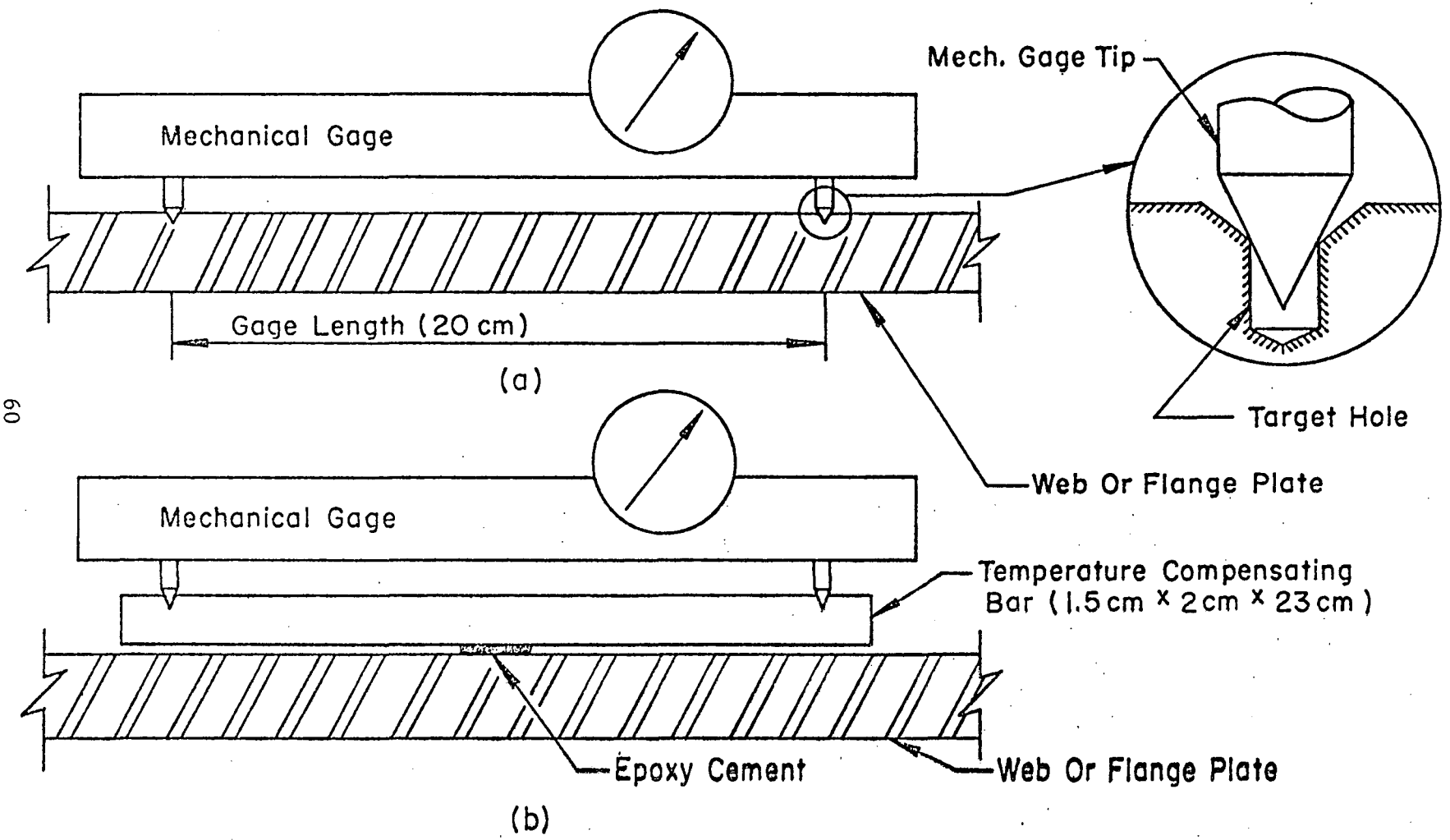

Fig. 9 Schematic of Mechanical Gage

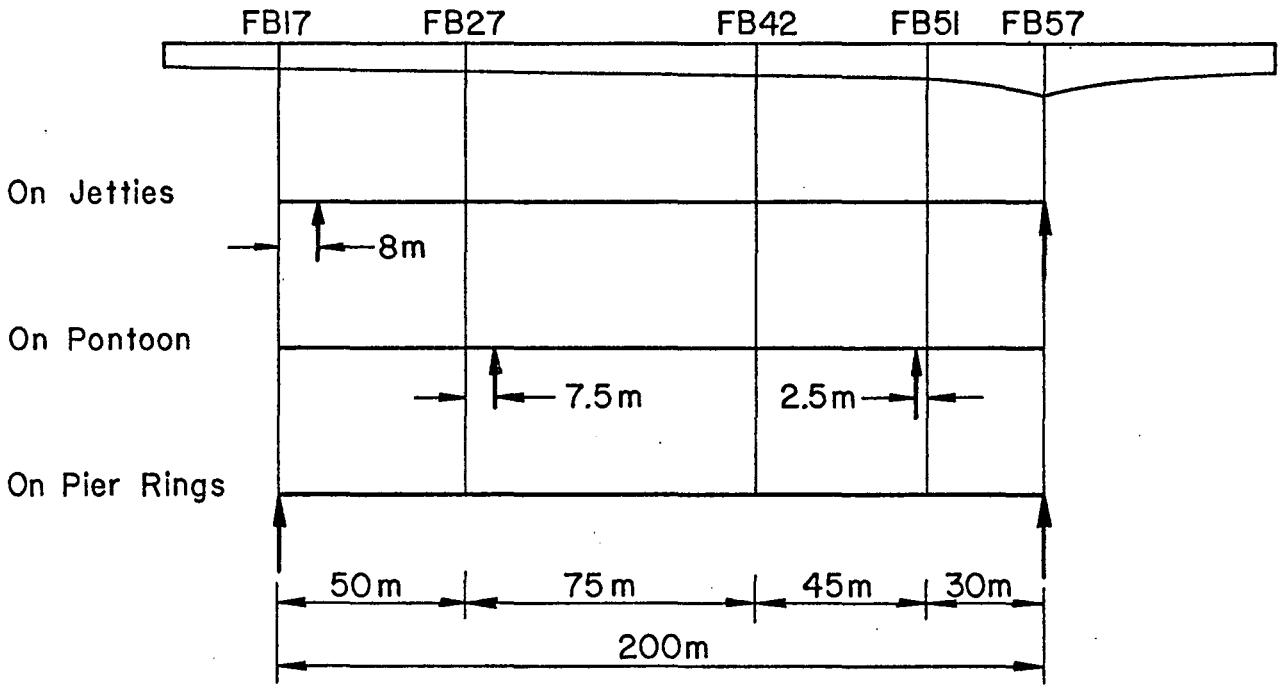

Fig. 10 Support Points - Rio Side Span Units

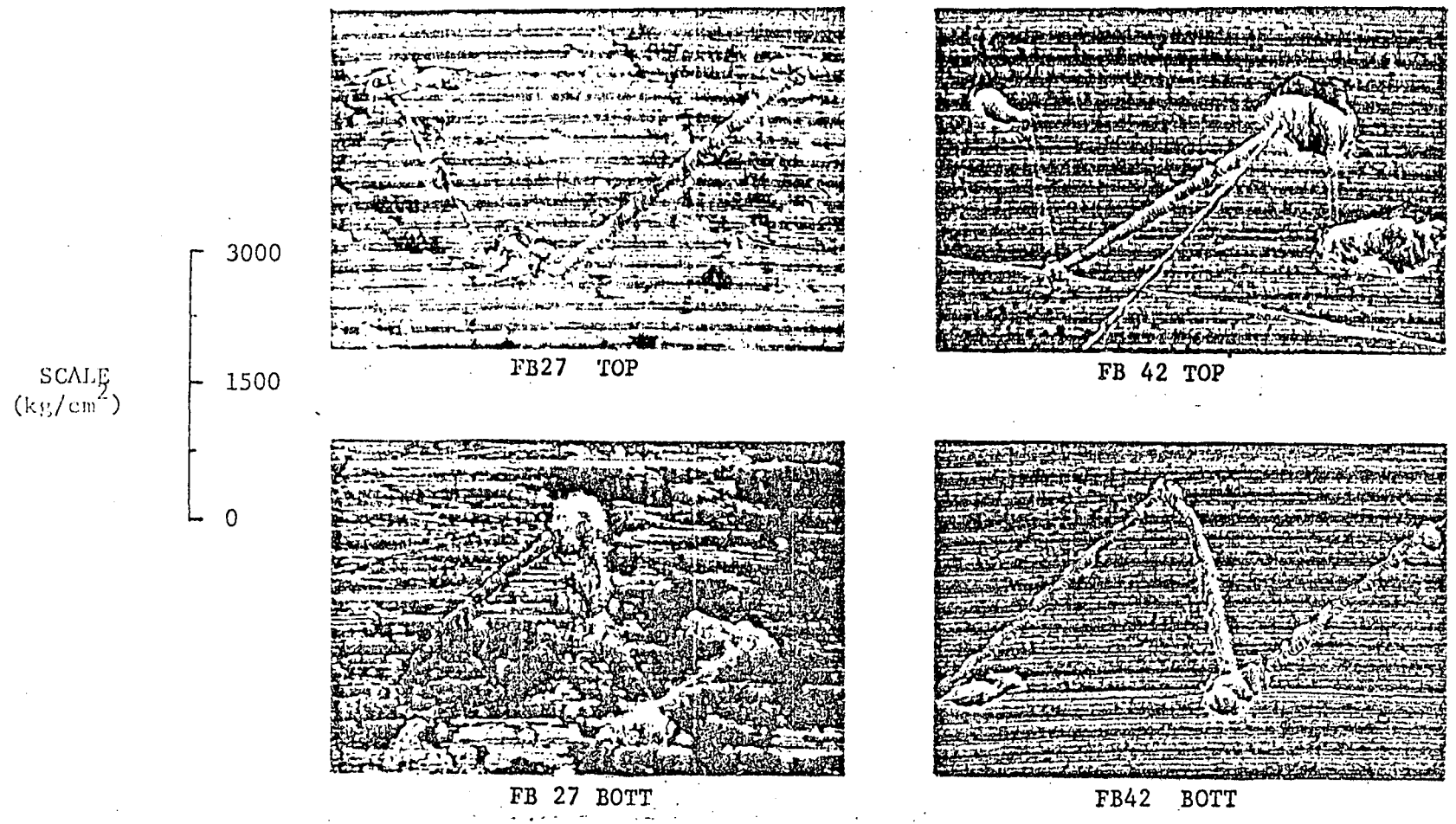

Fig. 11 SCRATCH GAGE TRACES (90X) - CONSTRUCTION STRESS CHANGES

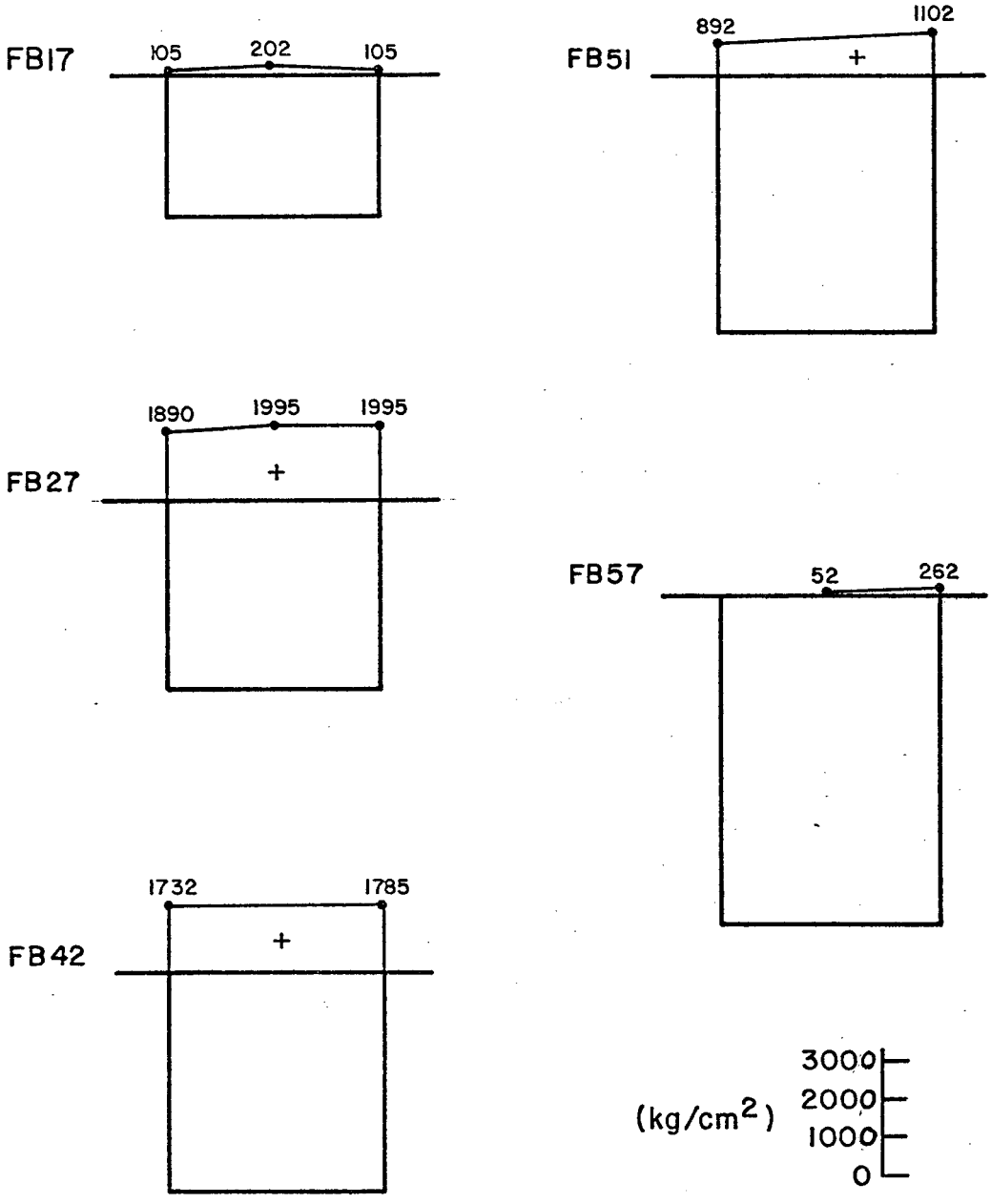

Fig. 12 Stress Changes (Mechanical Gage Measurements)-Jetties to Pontoon

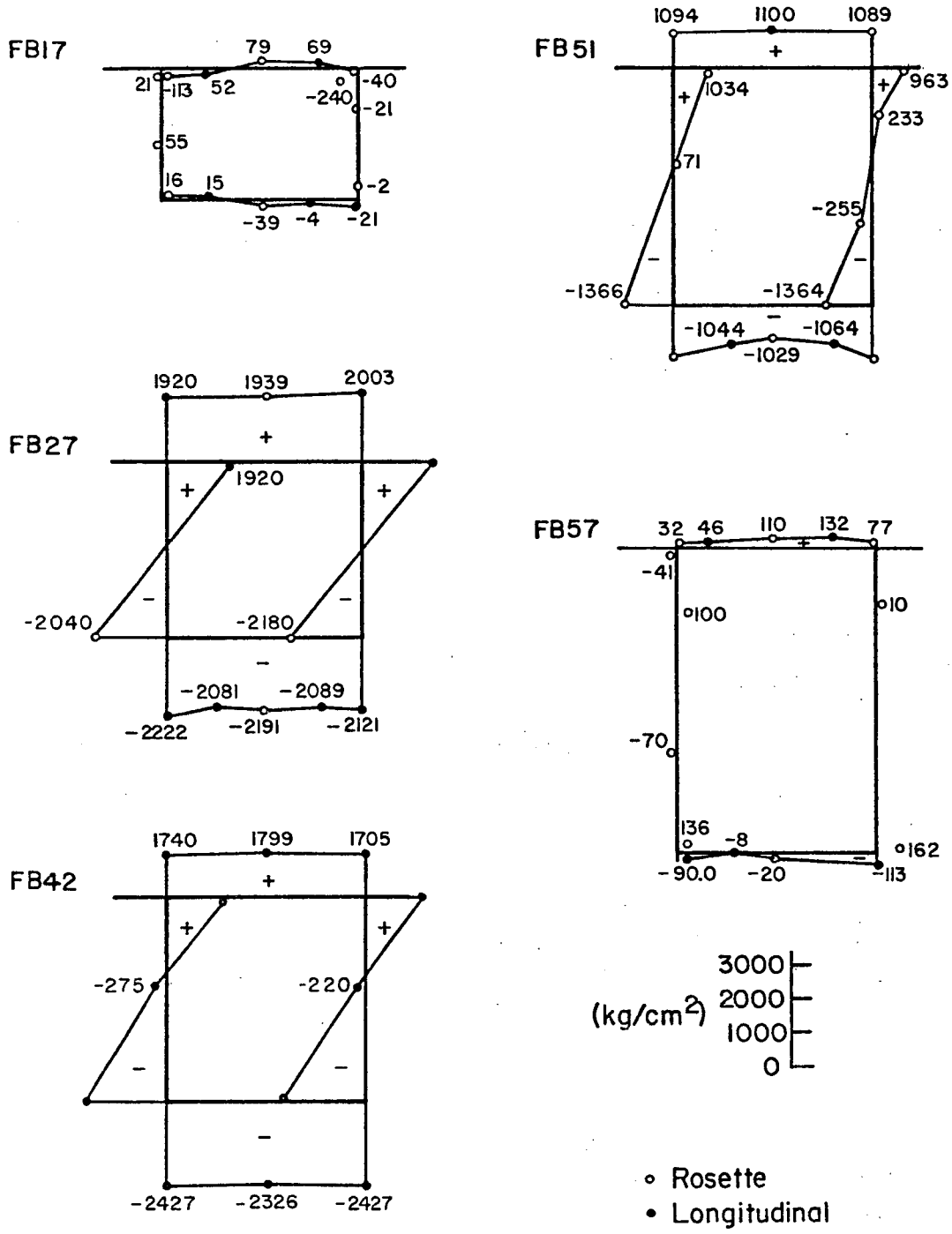

Fig.13 Stress Changes (Strain Gage Measurements) - Jetties to Pontoon

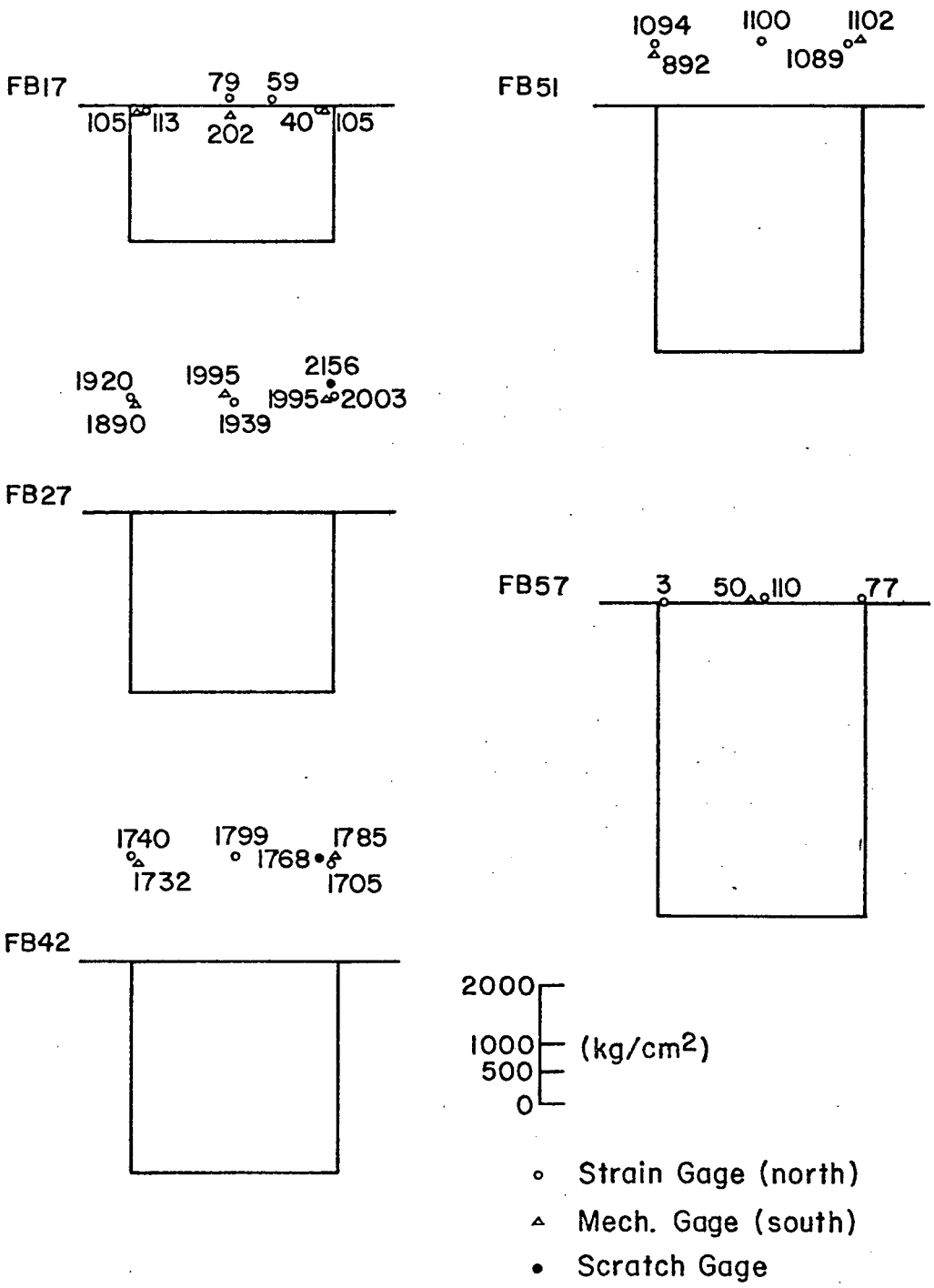

Fig. 14 Top Flange Stress Changes - Jetties to Pontoon
(Rio Side Span)

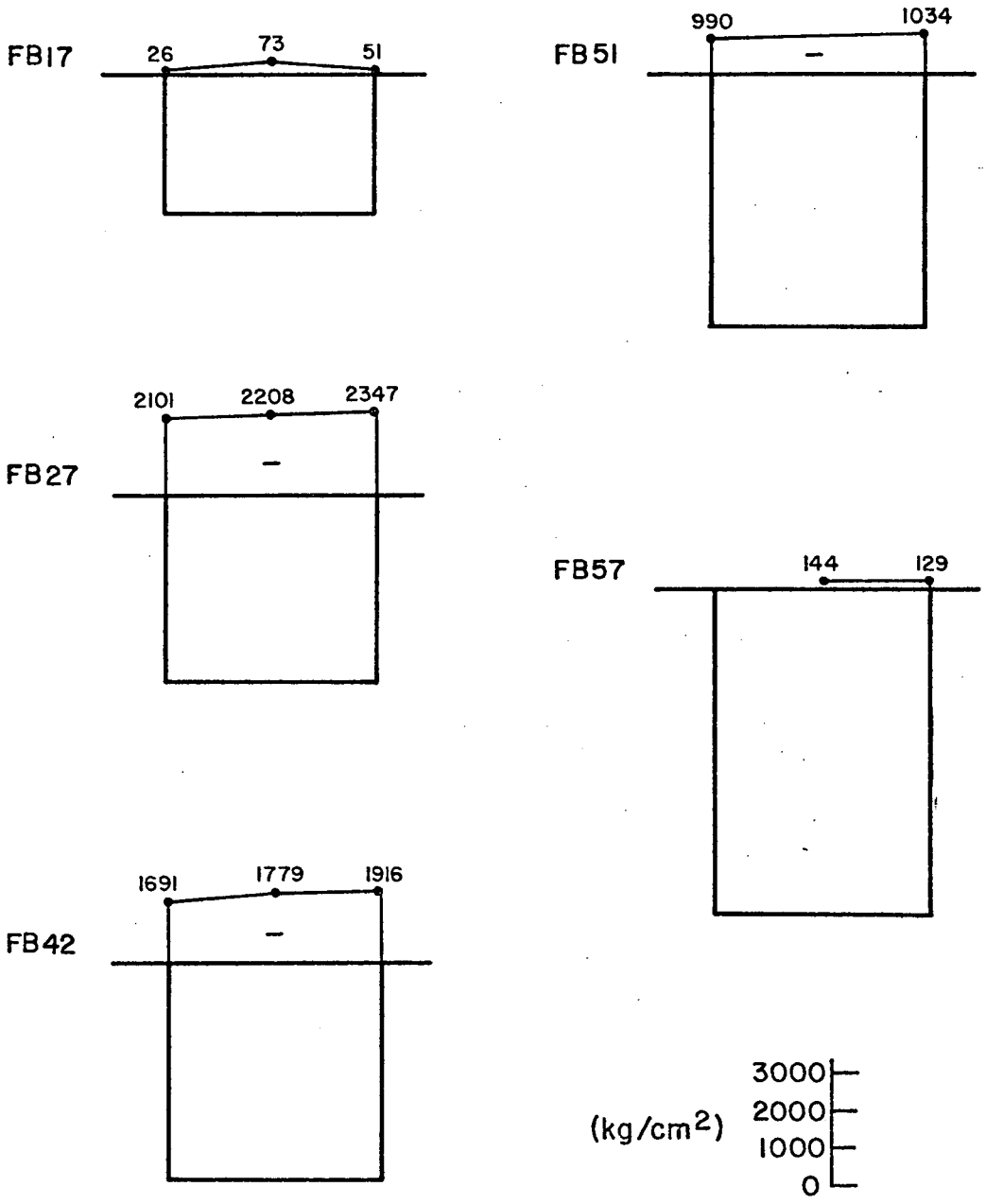

Fig. 15 Stress Changes (Mechanical Gage Measurements) - Pontoon to Piers

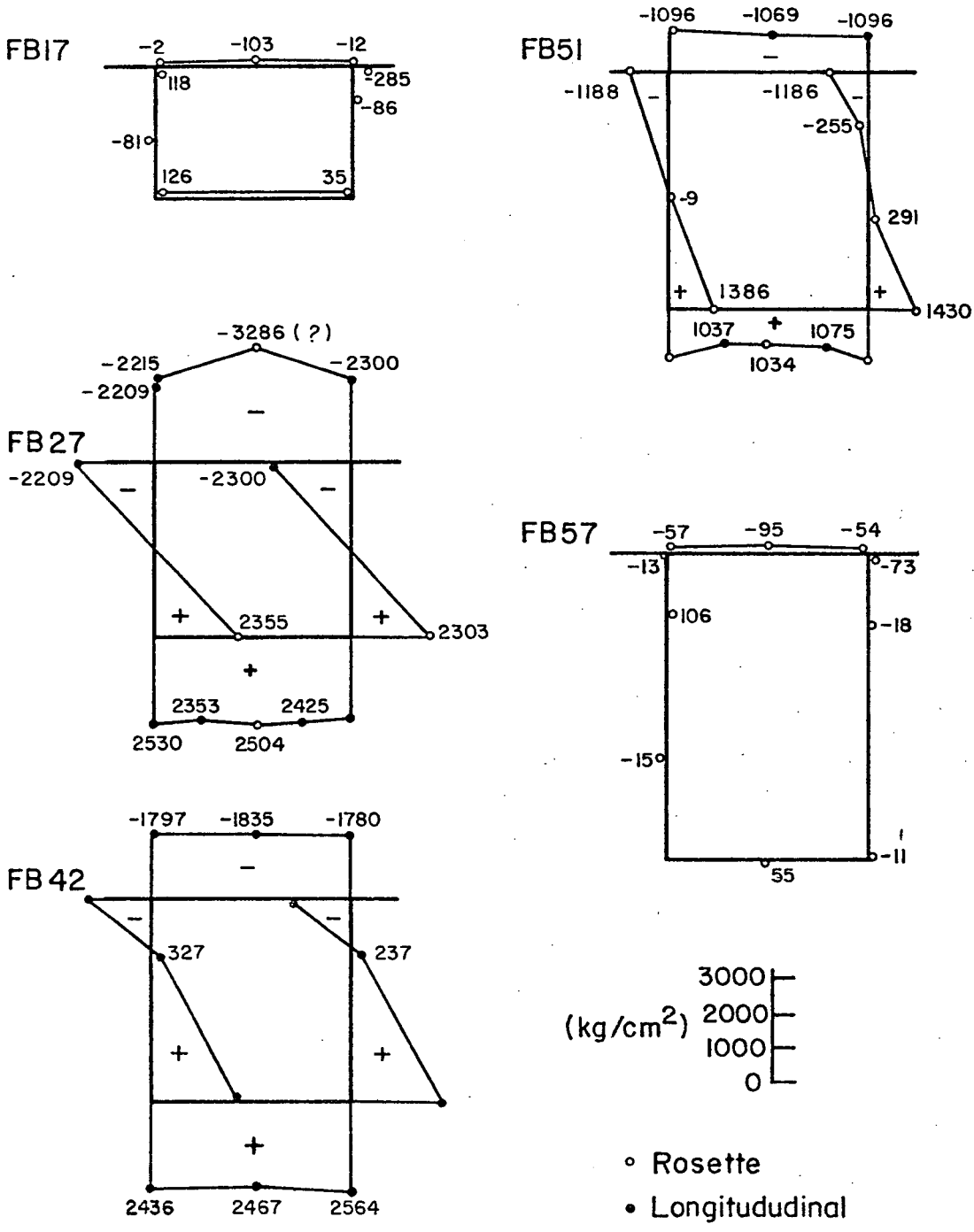

Fig. 16 Stress Changes (Strain Gage Measurements) - Pontoon to Piers

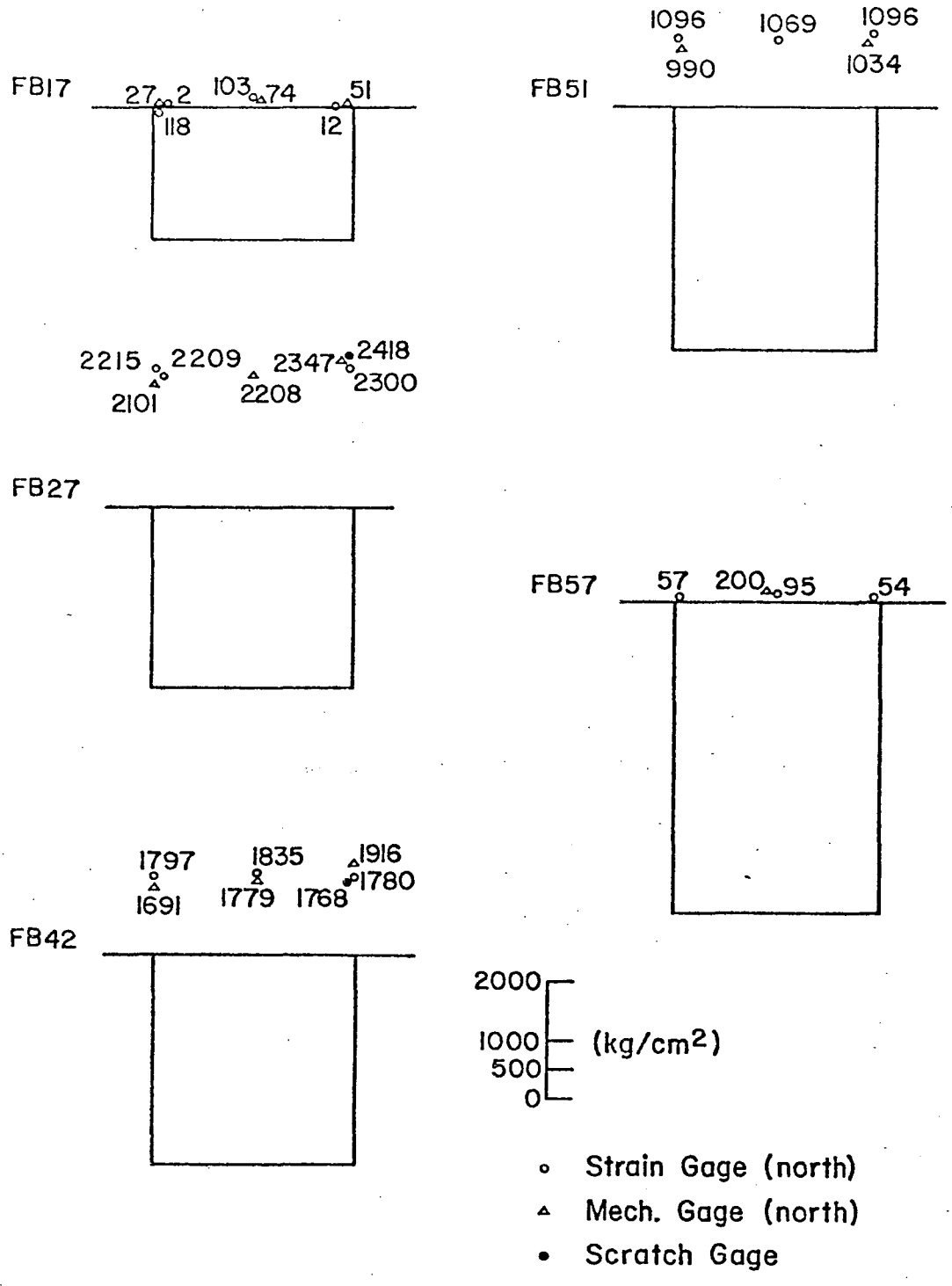

Fig. 17 Top Flange Stress Changes - Pontoon To Piers (Rio Side Span)

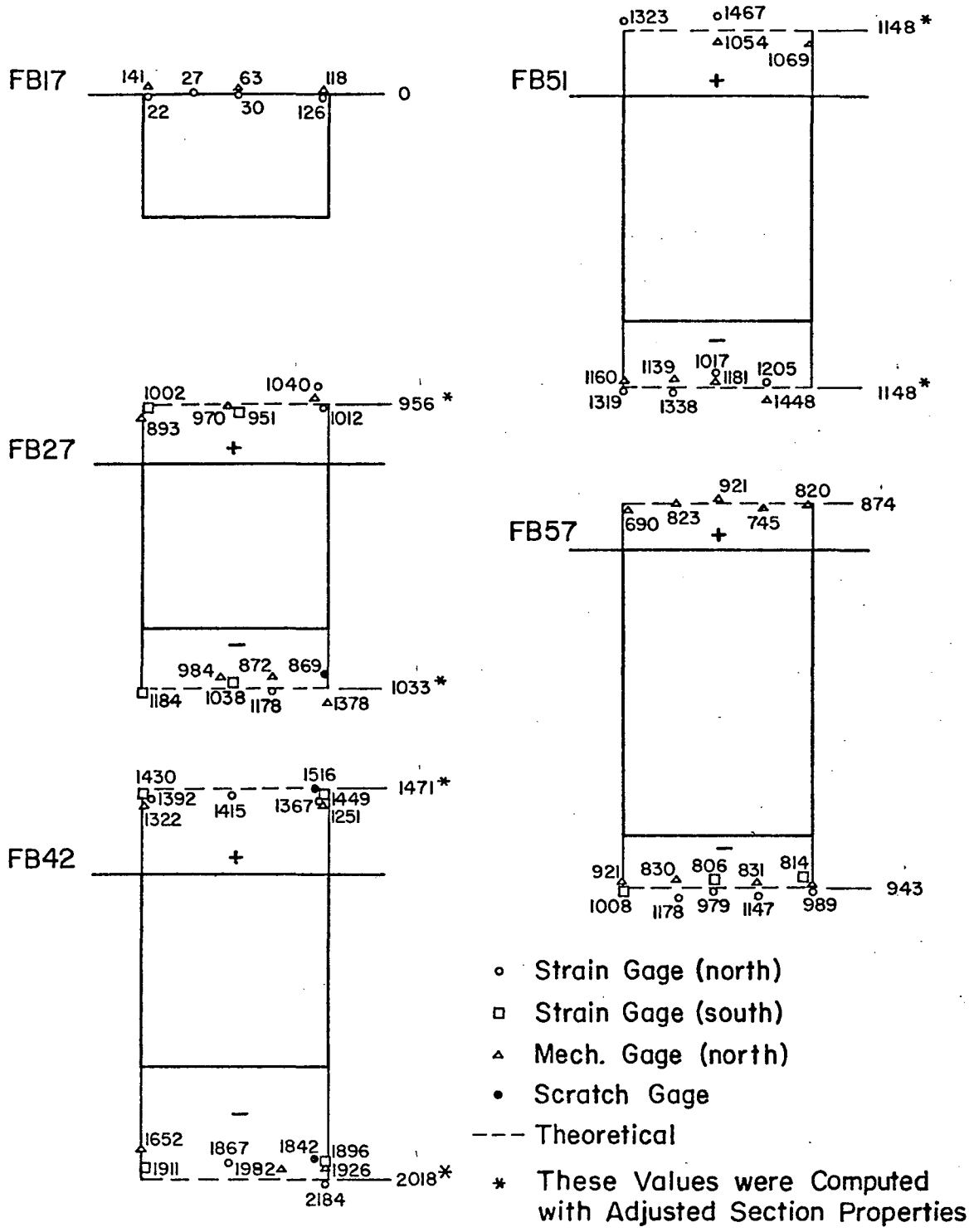

Fig. 18 Stress Changes - Center Span Lift

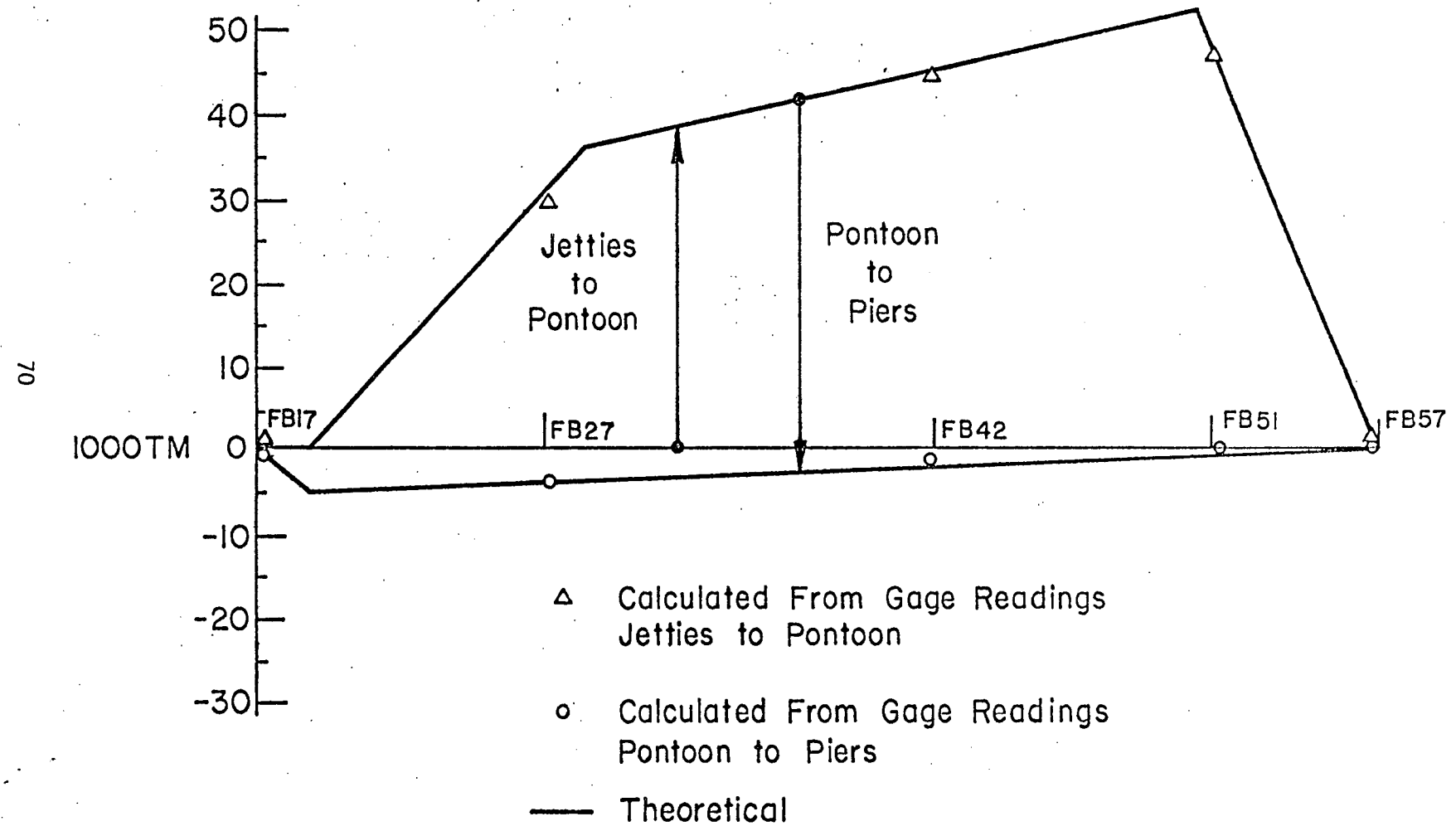

Fig. 19 Moment Changes - Rio Side Span Boxes

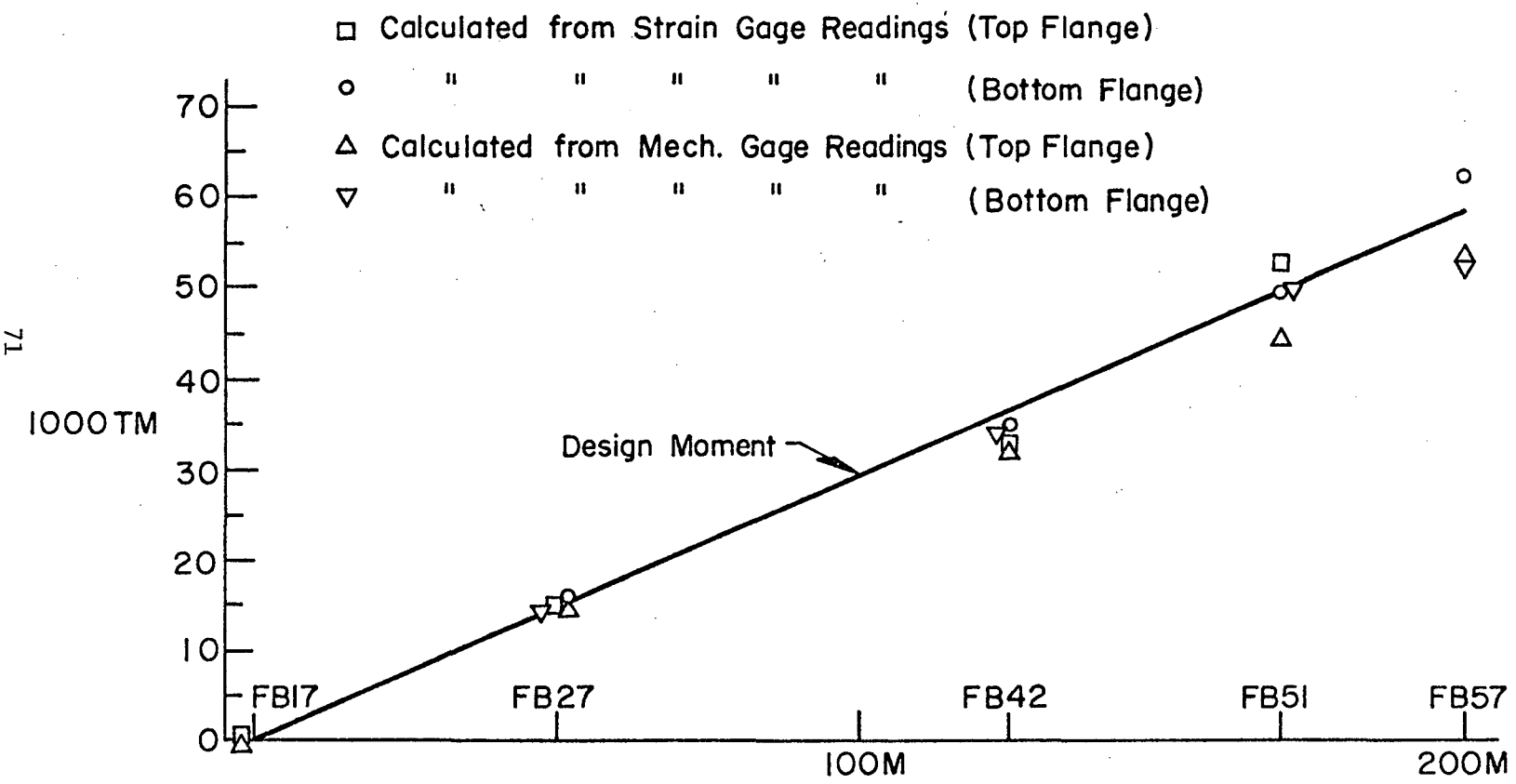

Fig. 20 Moment Change - Center Span Lift - Rio Side Span Boxes

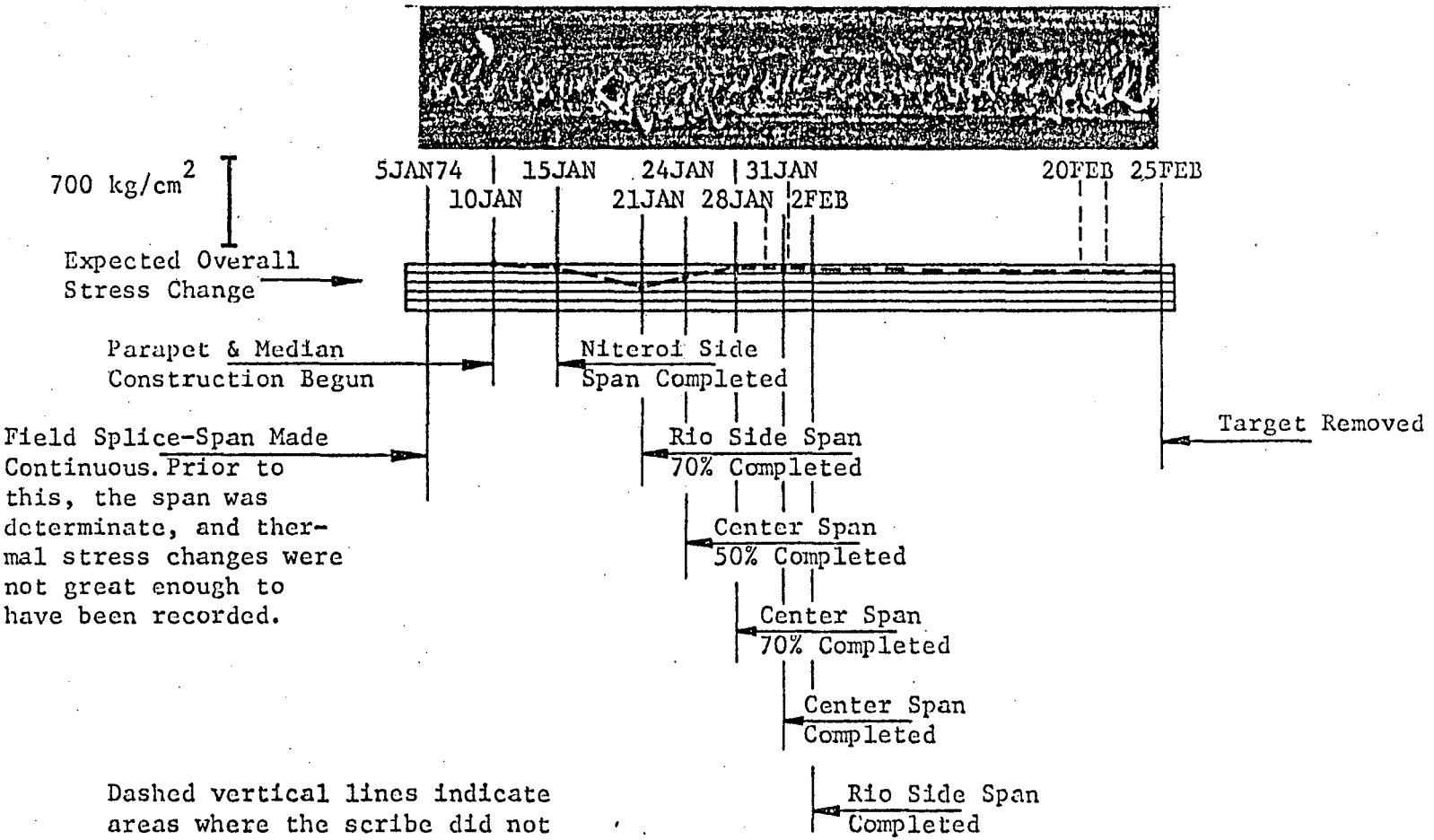

Fig. 21 Parapet and Median Construction - Scratch Gage Trace vs. Theoretical Values

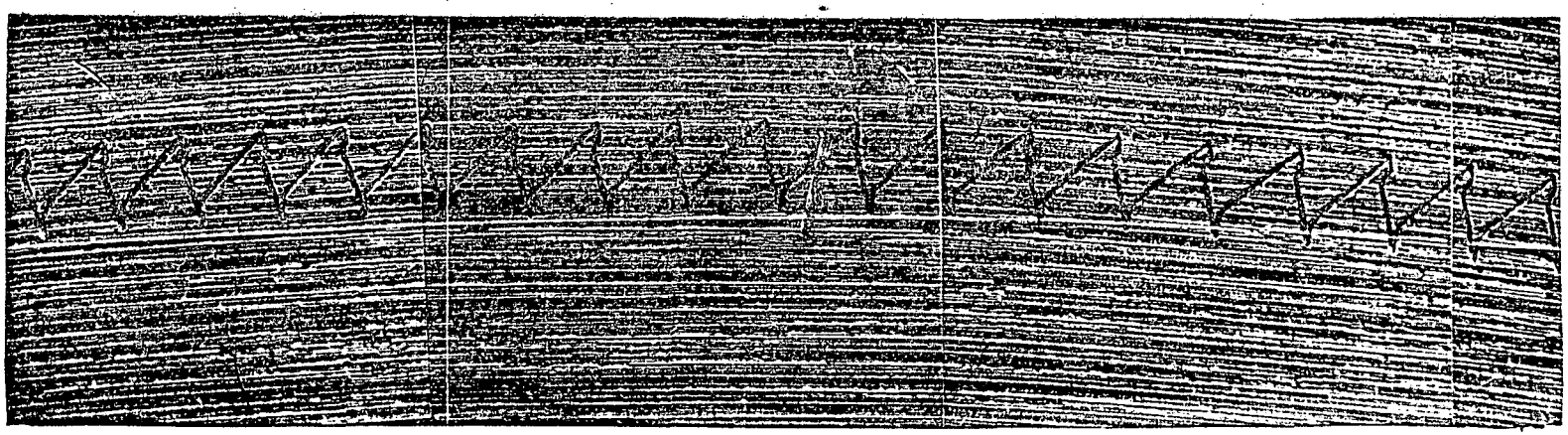

Fig. 22 Scratch Gage Trace

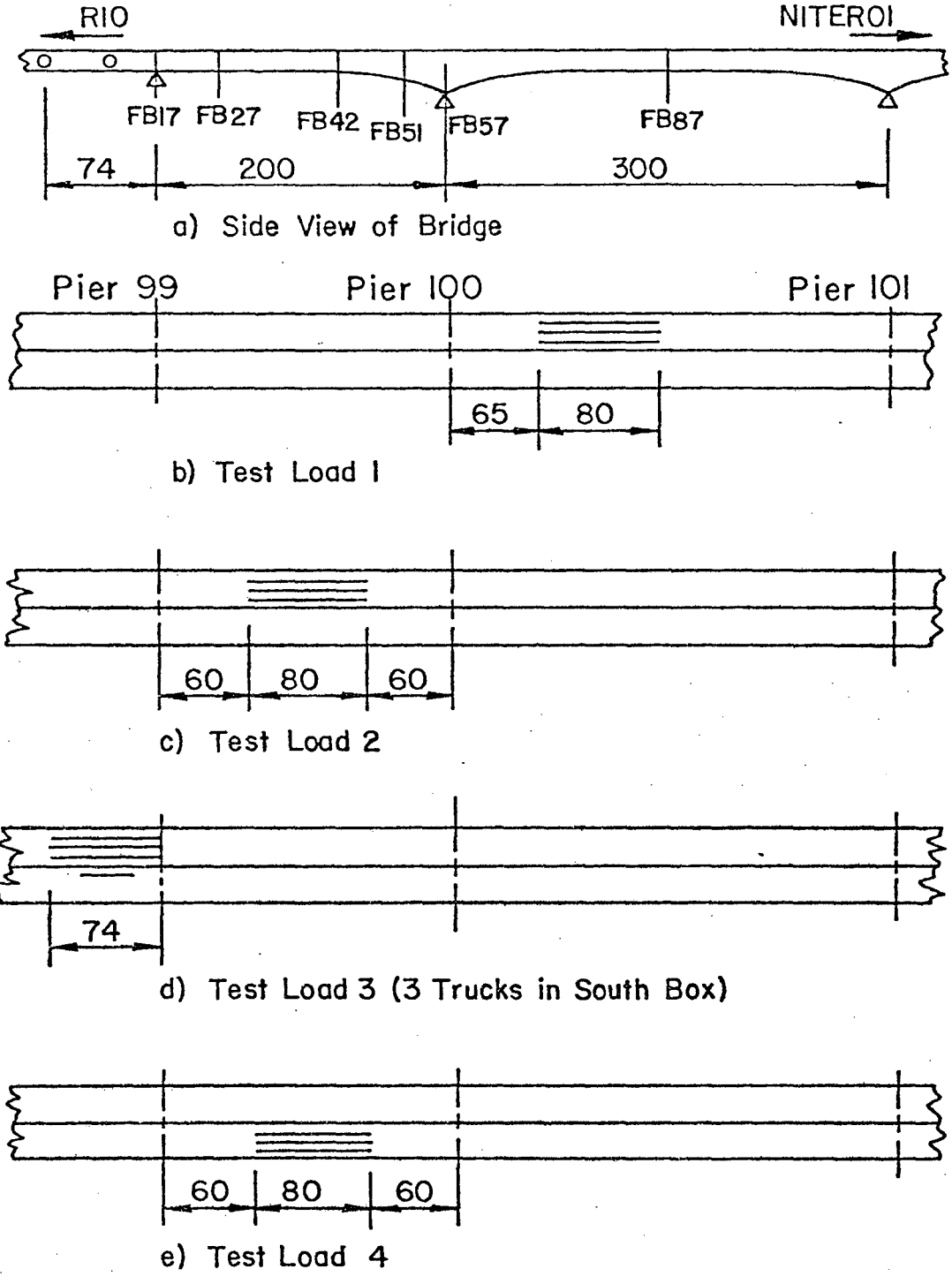

Fig. 23 Test Load Positions (21-17.5 Ton Trucks)
(All Dimensions in Meters)

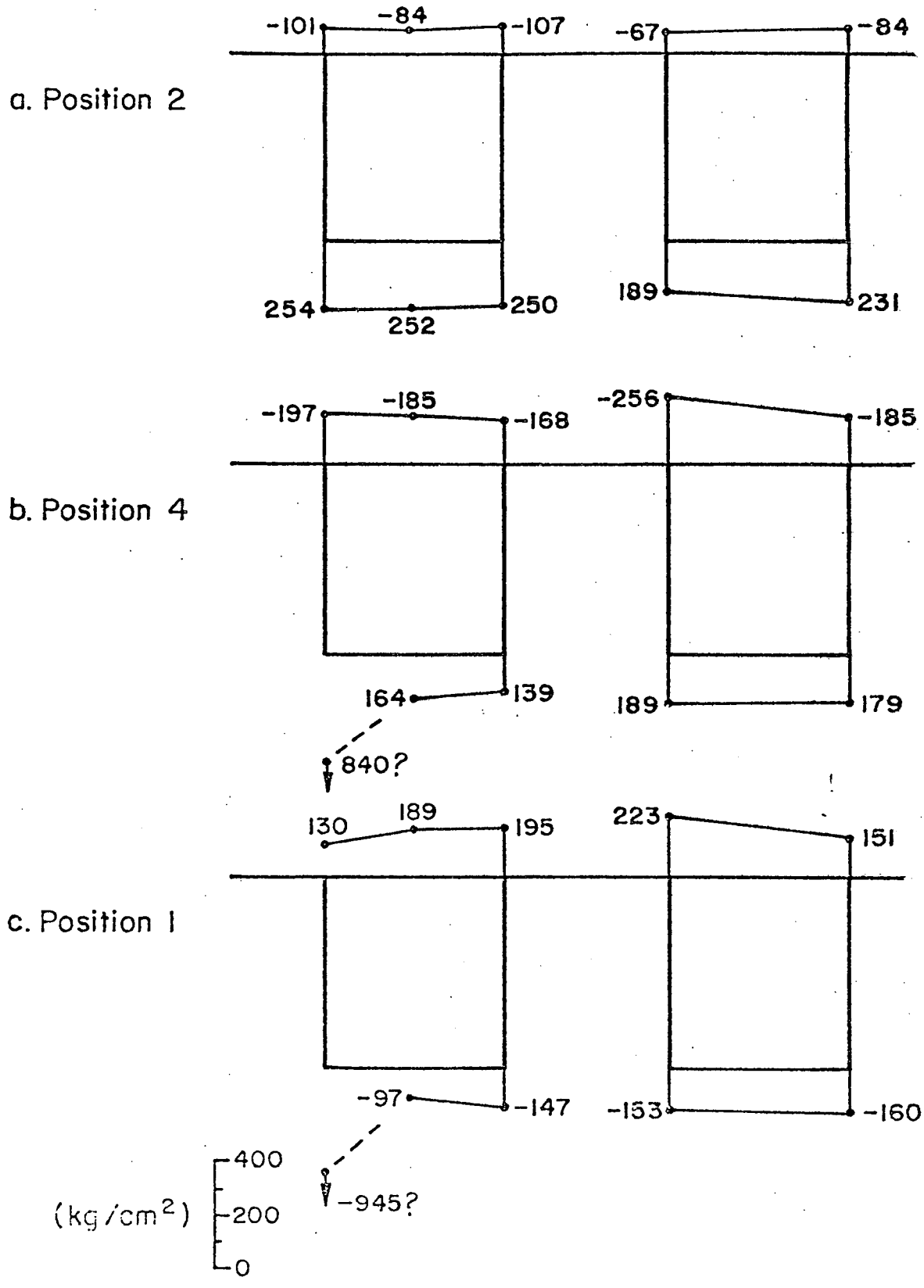

Fig. 24 Test Load Stress Changes

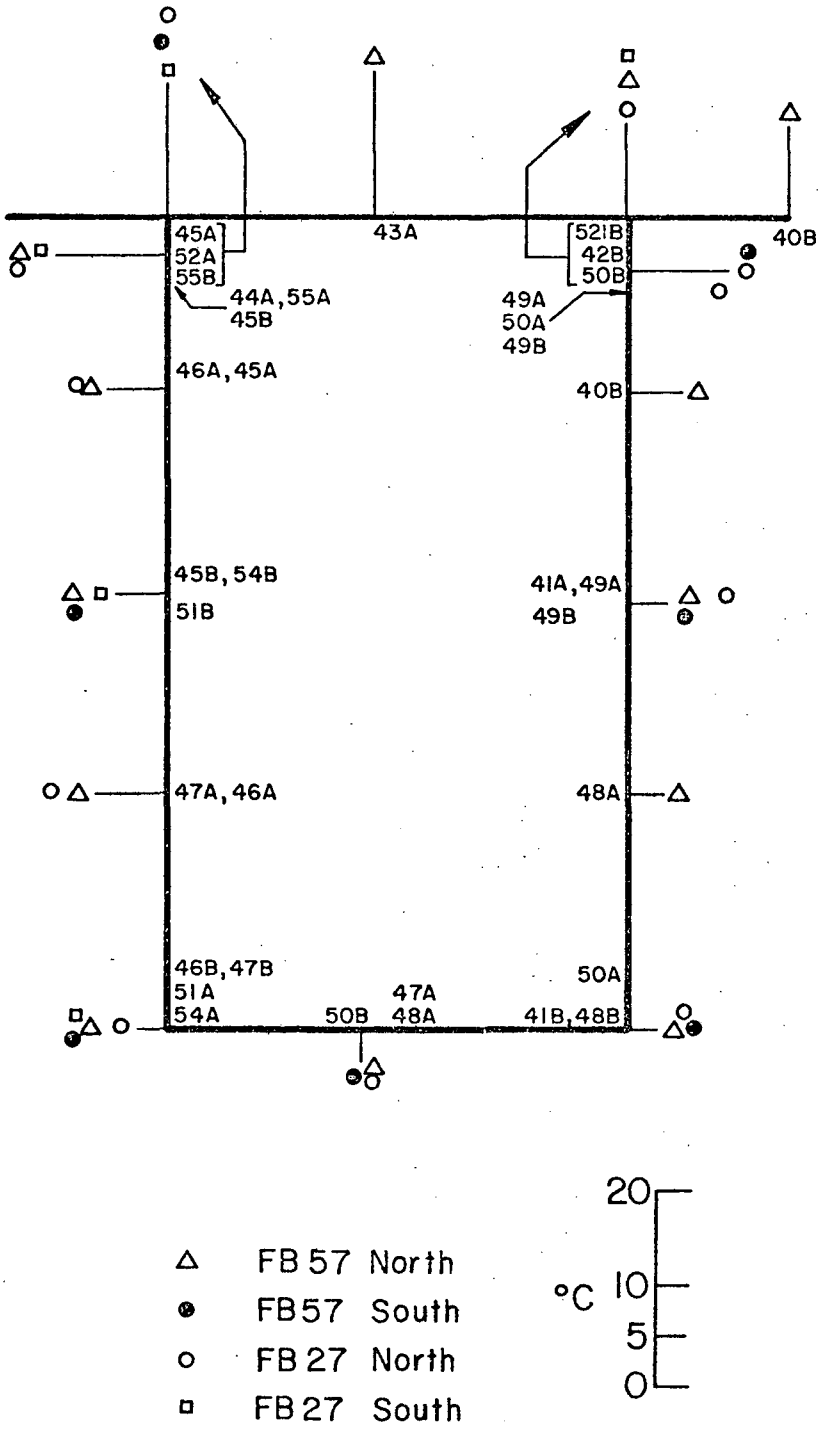

Fig. 25 Composite of Temperature Changes (16-17 January 1975)

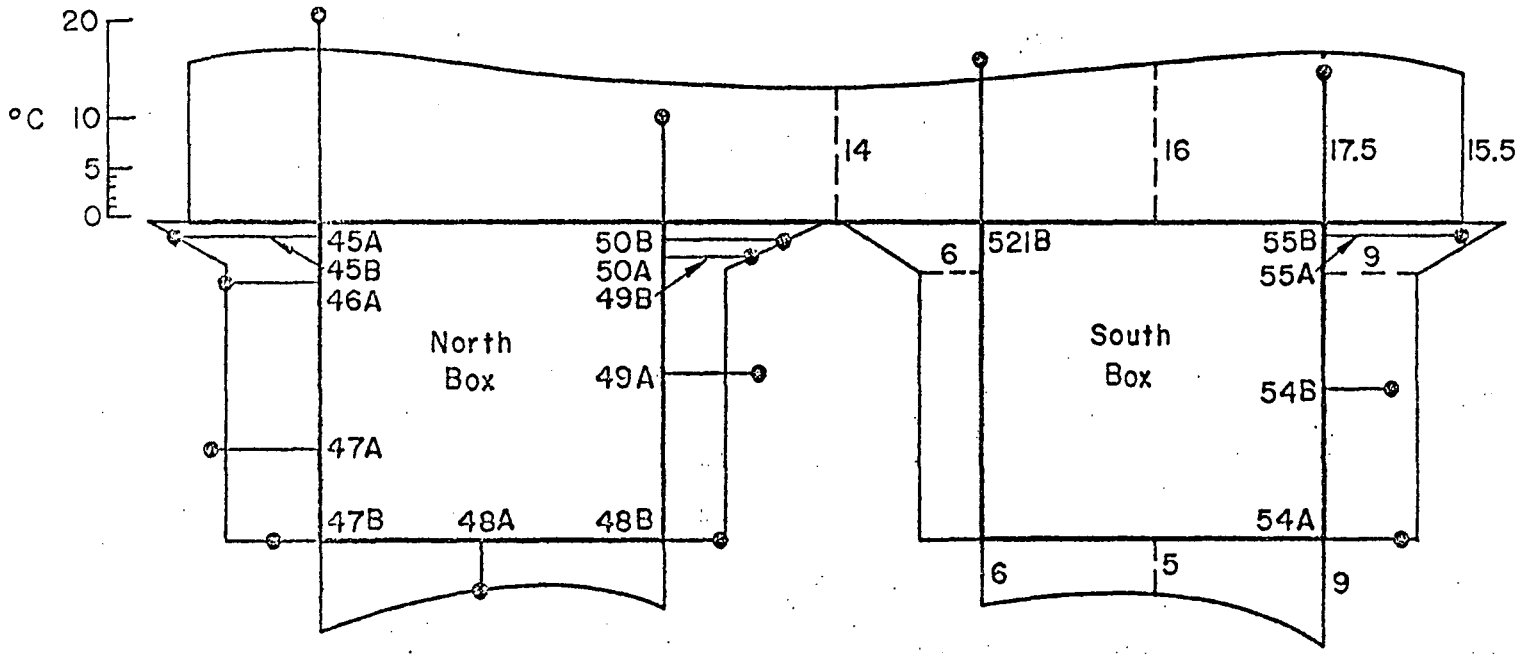

Fig. 26 Diurnal Temperature Change at FB27

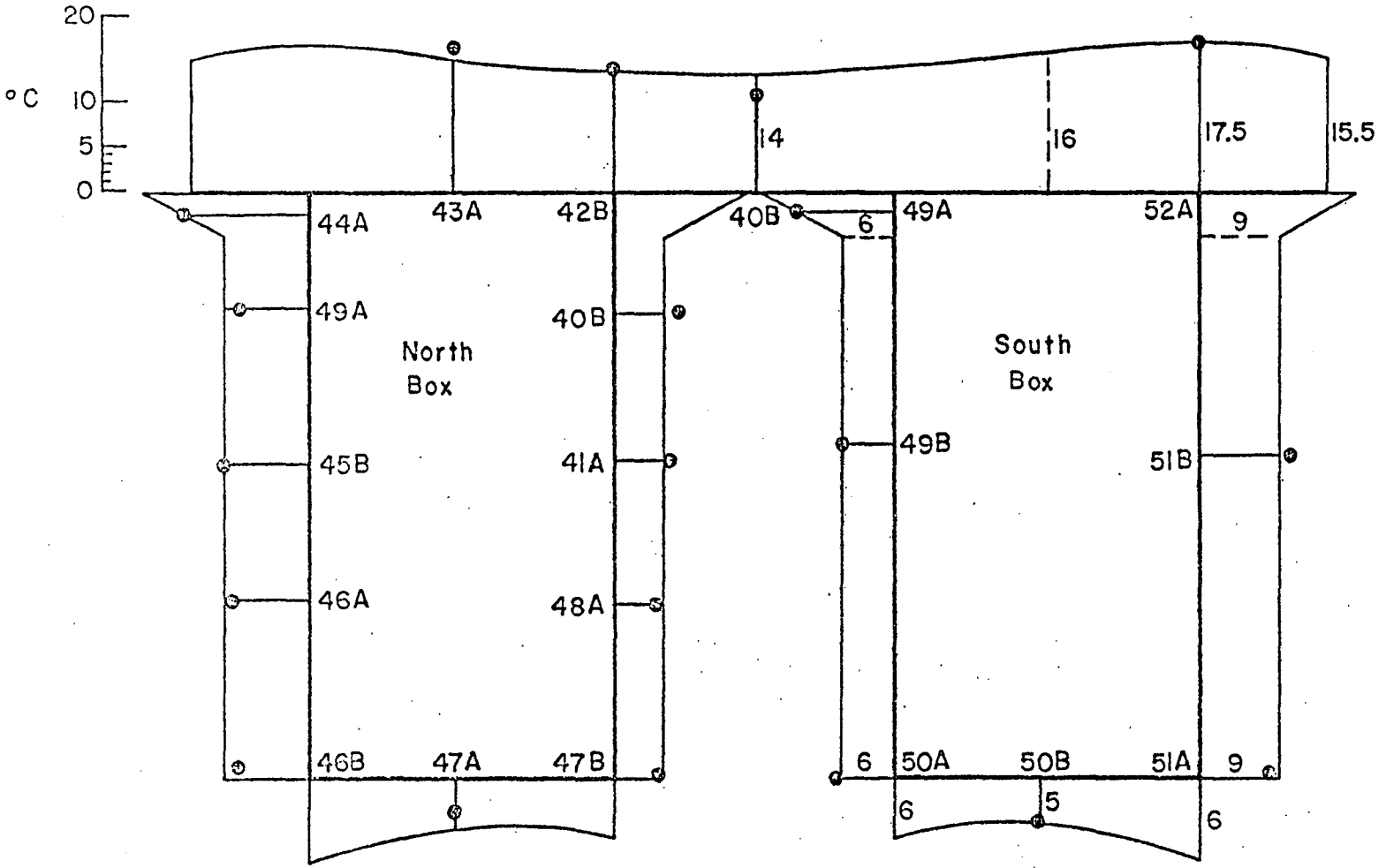

Fig. 27 Diurnal Temperature Change at FB57

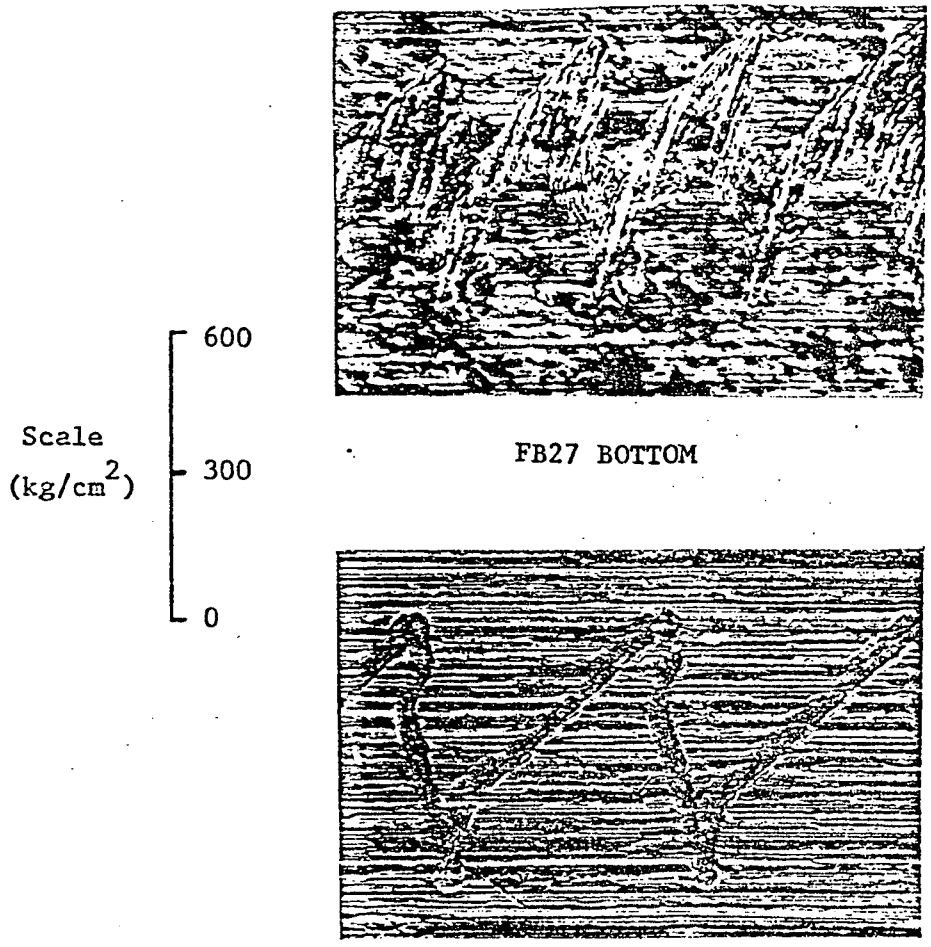

Fig. 28 Scratch Gage Traces (425X)
Maximum Thermal Stress Changes

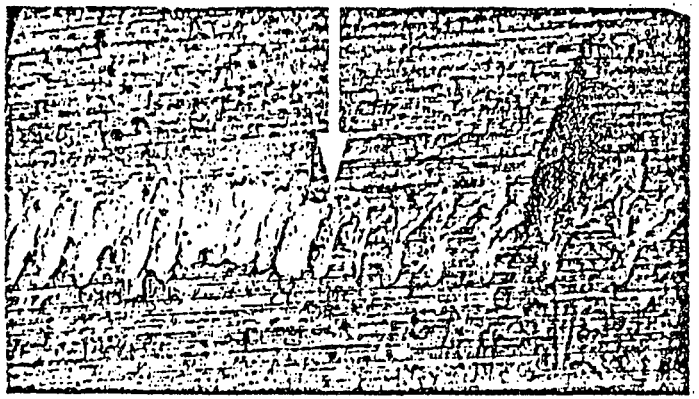

Scratch Gage Target No. 22
(A Portion)

Gage Length = 30.5 cm
Stress Change = 300 kg/cm^2
(At Arrow)

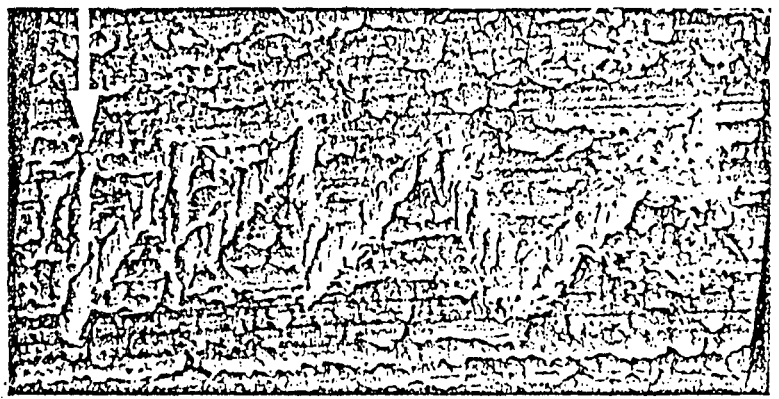

Scratch Gage Target No. 23

Gage Length = 100 cm
Stress Change = 205 kg/cm^2
(At Arrow)

Fig. 29 Comparison of Scratch Gage Traces for Different Gage Lengths
(Magnification = 210X)

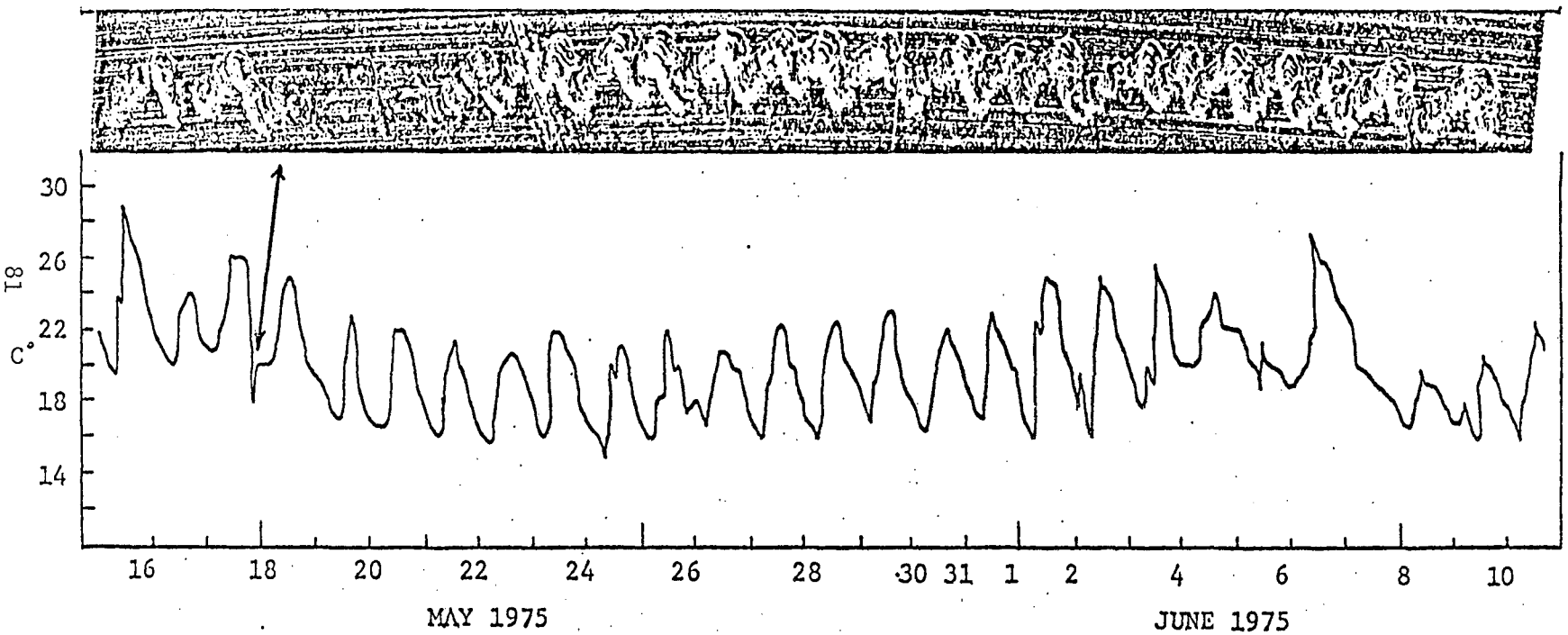

FIG. 30 SCRATCH GAGE TRACE (FB 42 BOTTOM) VS. AIR TEMPERATURE

REFERENCES

1. Prewitt Associates
   SCRATCH STRAIN (SSG) INSTALLATION MANUAL,
   Prewitt Associates, Lexington, Ky., 1972.

2. Mortlock, J. D.
   THE INSTRUMENTATION OF BRIDGES FOR THE MEASUREMENT OF TEMPERATURE AND MOVEMENTS, TRRL Report LR641,
   Transport and Road Research Laboratory, Crowthorne, Berks., 1974.

VITA

David H. DePaoli, son of Henry and Barbara DePaoli, was born October 7, 1951 in Palmerton, Pennsylvania. In June of 1969, the author graduated from Plymouth-Whitemarsh High School in Plymouth Meeting, Pennsylvania. In May of 1973, he received his Bachelor's degree from Lehigh University. From June 1973 to January 1974, he was employed as a structural designer by the Engineering firm of A. Ernest D'Ambly, Inc., Philadelphia, Pa. Since January 1974, the author has been attending Lehigh University taking courses toward a Master's degree, working half-time as a Research Assistant until September 1975, and as a part-time instructor since that date.